Modelling neuroimmune interactions using organotypic slice cultures

Buchule Mbobo

Submitted for the degree MSc in Medicine

Department of Pathology

Faculty of Health Sciences

University of Cape Town

13 March 2017

Supervisor: Prof Muazzam Jacobs

DECLARATION

I, Buchule Mbobo....., hereby declare that the work on which this dissertation/thesis is based is my original work (except where acknowledgements indicate otherwise) and that neither the whole work nor any part of it has been, is being, or is to be submitted for another degree in this or any other university.

I empower the university to reproduce for the purpose of research either the whole or any portion of the contents in any manner whatsoever.

Signed by candidate ...

Date: .....March 2017.....

Acknowledgements

I would like to express my gratitude to my supervisor Prof Muazzam Jacobs for making it possible for me to pursue this MSc degree and his continued support throughout this project. I wish to especially thank Dr JV Raimondo and Dr Nai-Jen Hsu for their tireless assistance, encouragement and support as my co-supervisors. Two really is better than one. Furthermore, the welcoming and supportive environment I experienced from the TB Group and Raimondo Lab was most valuable and appreciated, thank you.

Last but not least, my family. Ndiyabulela Ma ngengxaso no thando ondifudumeze ngalo, noku ndityhalela phambili ekufezekiseni amaphupha wam. Ku Mihlali no Xabakazi, ndiyabulela nakuni bantwana basekhaya ngoku ndigcina emandleni.

Enkosi.

Table of Contents

Figure List

Abbreviations

CNS-TB	– Central nervous system tuberculosis
EPTB	– Extrapulmonary tuberculosis
IL	– Interleukin
OBSCs	– Organotypic brain slice cultures
BCG-GFP	– Bacillus Calmette-Guerin-green fluorescent protein
RT	– Room temperature
ELISA	– Enzyme-linked immunosorbent assay
aCSF	– artificial cerebrospinal fluid
TTX	– Tetrodotoxin
M. tuberculosis	– *Mycobacterium tuberculosis*
Tuberculin PPD	– Tuberculin purified protein derivative
NMDA	– *N*-methyl-d-aspartate
MOI	– Multiples of infection
L. monocytogenes	– *Listeria monocytogenes*
CFU	– Colony forming units

Abstract

Tuberculosis predominantly manifests in the form of a pulmonary infection, but may spread out into other parts of the body and is then referred to as extrapulmonary tuberculosis (EPTB). One form of EPTB is an infection of the central nervous system (brain & spinal cord), CNS-TB. Although CNS-TB is relatively rare, accounting for about 5% of EPTB, it is characterised by high morbidity and mortality, particularly for children and immunosuppressed individuals.

To examine the effects of a *Mycobacterium tuberculosis* infection of neural tissue, researchers have hitherto relied on two animal models namely, *in* vivo intracranial infections or *in vitro* culturing with dissociated neural cells. Both models have yielded crucial insights concerning CNS-TB but each have limitations e.g. lack of access to the brain during infection *in vivo* and absence of the 3D organizational tissue structure *in vitro*. This study investigated the effect of the vaccine strain for tuberculosis, *Bacille Calmette-Guerin* (BCG) on neural tissue using the model of organotypic hippocampal slice cultures; an *in vitro* model that overcomes the previously mentioned obstacles. The study sought to expound on immunological and electrophysiological responses to the infection.

A viable and moderate BCG infection was established in the hippocampal slice cultures, confirmed by colony forming units enumeration and immunohistochemistry. However, immunological analysis using ELISA found that BCG infection did not change the production levels of cytokines and elicit a distinguishable immune response. To examine the neuronal function during BCG infection, whole-cell patch clamp technique was applied to the hippocampal slice cultures. The neuronal intrinsic properties were not significantly different between infected and non-infected slices. However, tuberculin PPD (*M. tuberculosis* extract) moderately and transiently had a depolarizing effect when ‘puffed’ directly onto neurons. In conclusion, organotypic slice cultures are suitable for the investigation of cellular interactions and neural functions in CNS-TB, and the neuronal impact of PPD warrants further investigation.

1. Introduction

1.1. Background

In 2014, an estimated 9.6 million people worldwide developed tuberculosis (TB) and approximately 1.5 million died from the disease, 400 000 of whom were HIV positive. In more detail, the 1.5 million fatalities comprised of 890 000 men, 480 000 women and 140 000 children. The *Global TB Report 2015* also showed that of the 22 high-burden countries, South Africa was one of the top six with between 400 000 – 510 000 incident cases recorded in 2014. Tuberculosis predominantly manifests in the form of a pulmonary infection, with extrapulmonary TB (EPTB) accounting for up to 20% of all reported cases. In South Africa the notified cases of EPTB for 2014 was recorded at 33 522. One form of EPTB is an infection of the central nervous system (brain & spinal cord), CNS-TB. In all reported cases of EPTB, about 5% are attributed to CNS-TB (Be et al., 2009) and despite its relative paucity, it is characterised by high mortality and morbidity; in particular to children (Farer et al., 1979) and immunosuppressed adults (Berenguer et al., 1992). This is most concerning given that South Africa suffers from HIV/AIDS infections at pandemic proportions (Figure 1).

1.2. Tuberculosis of the Central Nervous System

A person becomes infected with *M. tuberculosis* bacilli when they inhale aerosol droplets that contain the bacilli exhaled from an infected individual. In the lungs,

these bacilli infect and grow within alveolar macrophages. This active phase of bacterial replication i.e. progression of pulmonary disease, may continue such that the 'bacterial load' in the lungs spills over into the local blood stream. In the blood the bacteria may disseminate to other systems or organs in the body including the immune privileged CNS (Donald et al., 2005, Rock et al., 2008). CNS-TB develops as *M. tuberculosis* bacilli are deposited in the meninges, brain parenchyma or spinal cord following haematogenous dissemination to form small tuberculous foci ("Rich foci") (Rich and McCordock, 1933).

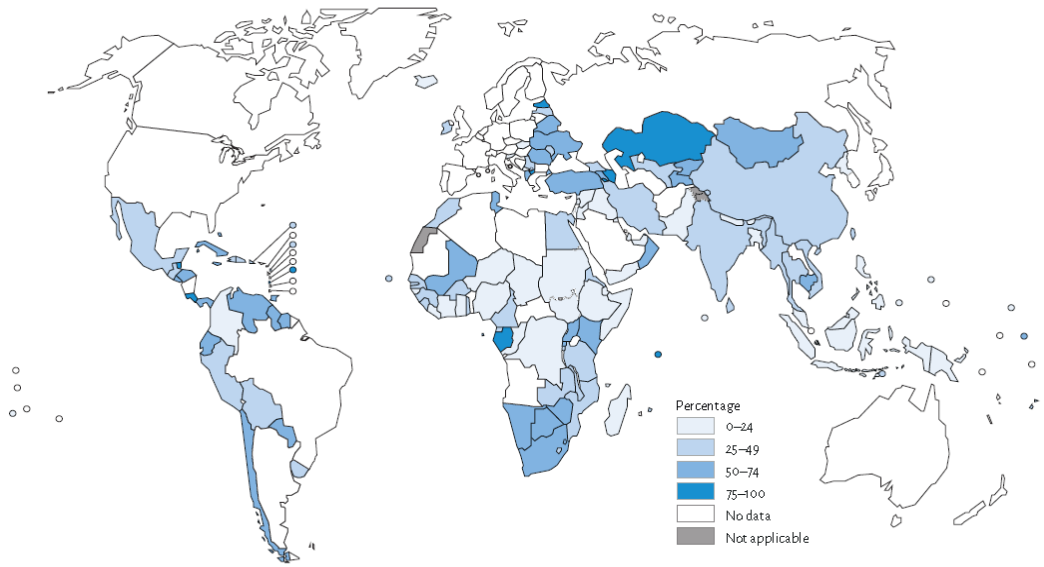

Figure 1: Number of HIV-positive TB patients on antiretroviral therapy (ART) as a percentage of estimated HIV-positive incident TB cases in 2014[a]

[a] includes all notified new, relapse and non-relapse retreatment cases (numerator). The denominator (i.e. estimated HIV-positive incident cases) includes new and relapse cases only

These foci expand to form granulomas/tuberculomas, which at some later stage, physically rupture and thereby directly spread bacilli into the cerebral spinal fluid

(CSF) within the subarachnoid space which eventually causes tuberculous meningitis. As mentioned earlier, bacterial infections of the CNS disproportionately affect human beings during childhood i.e. from neonatal to primary school age children. Furthermore, the characteristic high morbidity, if death is avoided, will in 50% of all cases result in permanent neurological sequelae (Bedford et al., 2001, Merkelbach et al., 2000, Grimwood et al., 2000).

1.3. Neuroinflammation

Neuroinflammation is the term used to describe an immune response in the CNS that may be elicited by a pathogen, physical trauma, toxins and/or pathological neural tissue degeneration. In the CNS, the microglia as the resident phagocytic cells are the key mediators that induce and regulate the immune response (Rock et al., 2004). Prior to the presence or occurrence of an inflammation-stimulating event, the microglia are in a resting (ramified) state i.e. an inactivated state, but they maintain surveillance and housekeeping of the tissue environment (Nimmerjahn et al., 2005). Hence the activation of microglial cells, in general, is viewed to be the principal hallmark of inflammation in the CNS (Kreutzberg, 1996).

During infection, the mycobacteria preferentially infect microglia (Curto et al., 2004, Rock et al., 2005), counter intuitively, as an evasion stratagem whereby instead of being cleared, the bacteria productively grow within the microglia. This manoeuvre is similar to the evasion mechanism employed by *M. tuberculosis* when it primarily infects alveolar macrophages to secure productive growth during pulmonary infection (Bermudez and Goodman, 1996). This apparent ‘susceptibility’ of microglia to bacterial colonization is attributed to their similarity with monocytes as

their progenitors share primitive origin in the mesoderm that seed both the brain parenchyma and pulmonary tissue during early development (Hess et al., 2004). However, some studies have suggested that microglia may function as an independent, self-regenerating population post-seeding during foetal development through to adulthood (Ginhoux et al., 2010). The latter view also highlights the singular importance of microglia as the major innate immune cells in the CNS that provide protection of the brain without a significant reliance on mononuclear cells from the periphery (Spanos et al., 2015). The importance of microglia notwithstanding, other CNS cells such as astrocytes, play a contributive role in the innate immune response, and even traditionally non-phagocytic neurons have also been shown to internalize *M. tuberculosis* bacilli (Rock et al., 2005, Randall et al., 2014, Dong and Benveniste, 2001). So collectively this demonstrates that the innate immune response in the CNS involves the major constitutive cell types. The inflammatory immune response elicited by *M. tuberculosis* infection naturally involves a myriad of pro-inflammatory cytokines & chemokines that are differentially secreted by immune effector cells such as microglia and infiltrating macrophages & $CD4^+$ T cells. These immune mediators include interleukin-6(IL-6), interferon gamma (IFN-γ), CCL2, CCL5, IL-1β and tumour necrosis factor alpha (TNF-α) which all play a role in granuloma formation, neuropathogenesis and protective immunity during CNS-TB (Curto et al., 2004, Tsenova et al., 1999, Rock et al., 2005, Lee et al.).

1.4. Neurological Activities and Deficits

The neurological deficits that manifest during an infection and also following successful treatment of bacterial infections in the CNS, directly implicate collateral

parenchymal tissue damage as the major cause. The aberrant behavioural and cognitive changes observed from sick and recovered patients, to a significant degree point to the area or distinct anatomical structure that has incurred damage pursuant to inflammatory response clearance and/or drug treatment of the infection (Perny et al., 2016). The abnormal outcomes from the infection include visual impairment, hearing loss, epilepsy, depressed cognitive/intellectual ability and abnormal behaviour (Perny et al., 2016, Nataprawira et al., 2016, Hosoglu et al., 2002, Grimwood et al., 1995, Lucas et al., 2016). The aforementioned sequelae from a CNS bacterial infection may persist in the short or long term. And correspondingly, the time period for recovery reveals the differential repair and/or poor regenerative capabilities of the neuronal tissue. Therefore it is important to investigate how an infection affects the properties and function of neuronal cells i.e. the impact on their physiology.

1.5. Neurophysiology

In the central nervous system, which can be broadly described to be constituted of glial and neuronal cells, the transmission of signals or 'information' is the primary function and domain of neurons. It therefore can be reasoned that it is a disturbance in the signalling of neurons that result in observable deficits in brain function. Neurons are generally characterised as 'excitatory' when they release the neurotransmitter glutamate or 'inhibitory' when they release the major inhibitory neurotransmitter, γ-aminobutyric acid (GABA) (Megias et al., 2001). The glutamate released by excitatory neurons binds to glutamate receptors on the postsynaptic cell, resulting in the influx of positive ions and depolarization of the membrane (a

positive shift in membrane potential) i.e. excitatory neurons causes excitatory postsynaptic potentials (EPSPs). In contrast the GABA released by inhibitory neurons binds to and opens $GABA_A$ receptors which cause chloride ion (Cl^-) influx and membrane hyperpolarization i.e. inhibitory neurons cause inhibitory postsynaptic potentials (IPSPs). When the neuronal membrane potential or voltage exceeds a certain threshold value called the action potential threshold, voltage-gated sodium channels open representing the start of a rapid wave of depolarization termed an action potential.

When an action potential, traveling along the axon of the presynaptic cell reaches the terminus i.e. the active zone, it causes the synaptic vesicles to fuse with the cell membrane and thereby release neurotransmitter into the synaptic cleft (Burns and Augustine, 1995). The neurotransmitter traverses the short distance of the cleft and binds to receptors on the postsynaptic density (surface) of the postsynaptic cell. The extent to which neurotransmitter release and receptor activation at the synapse modifies the postsynaptic potential and the ease and frequency at which action potentials are generated is a function of several neuronal properties collectively termed 'intrinsic properties'. These include the neuronal membrane resistance and capacitance, which determine the magnitude and time course of the membrane potential changes in response to synaptic currents. The membrane resistance and capacitance are a cumulative property of the size of a neuron and the density/type of passive ion channels in the membrane. Furthermore, intrinsic properties relate to the action potential threshold and the maximum frequency that a neuron is able to generate action potentials. These properties are set by the density and function of the voltage-gated sodium (Na) and potassium (K) channels (Beck and Yaari, 2008). Collectively then, neuronal intrinsic properties dictate how neurons integrate their

synaptic inputs to generate outputs and hence are fundamental to the function of individual cells and by extension the brain.

1.6. Hippocampus: structure and function

The hippocampus can be divided into 3 basic regions: the dentate gyrus (DG), CA3 and CA1 pyramidal neurons(Christie and Cameron, 2006) (Figure 2). These three regions form a local circuitry with granule neurons in the DG having axonal processes that synapse with CA3 pyramidal neurons, which in turn form synapses with CA1 pyramidal neurons (Christie and Cameron, 2006, Leuner and Gould, 2010). The CA1 pyramidal neurons then transmit the signal out of the hippocampus.

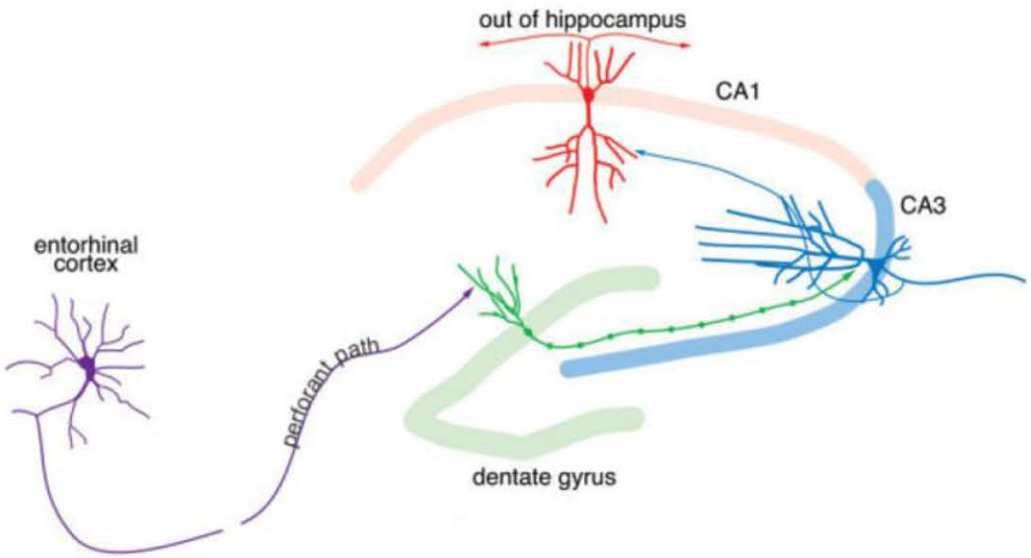

Figure 2: A schematic diagram of the basic tri-synaptic circuit of the hippocampus showing axons of granule neurons (DG) synapse on CA3 pyramidal cells, which in turn synapse onto CA1 pyramidal cells, which then send their axons out of the hippocampus (Christie and Cameron, 2006)

The CA3 and CA1 pyramidal neurons are generally characterised as excitatory (Megias et al., 2001) with a resting membrane potential of approximately -60mV.

The easily identifiable structure of the hippocampus and the known properties of its neurons make it an ideal structure to use as a model to study neural activities in the brain.

1.7. A Model: Organotypic Slice Cultures

Studies that hitherto have been conducted to determine various aspects of *M. tuberculosis* infection of the CNS have included both *in vitro* and *in vivo* methodologies. The *in vitro* experiments typically involve the culturing of dissociated cells on media plates, where they are then incubated with *M. tuberculosis* bacilli. The *in vivo* methods generally involve an intracranial or intravenous injection of *M. tuberculosis* bacilli into an animal, followed by harvesting and fixing of tissues for analysis using molecular techniques (Randall et al., 2014, Be et al., 2008)**.** These experimental preparations have yielded important insights into the pathogenesis of CNS-TB. However, both preparations exhibit significant limitations namely that, dissociated cell cultures disrupt normal tissue architecture and cross cell-type cellular interactions, and *in vivo* injection followed by brain fixation does not allow for the observation or measurement of dynamic neuroimmune interactions nor neuronal function *in situ*.

These significant shortcomings of the traditional investigative methods have necessitated the search for another model to study infections of the CNS and more specifically CNS-TB. One such methodology is to use organotypic brain slice cultures (OBSCs). An organotypic slice culture is an *in vitro* methodology where a particular brain region or structure typically from murine or rat neonates is sectioned into 300-400µm thick slices that are maintained on porous membrane inserts in

culture for a period of several weeks to a month (Stoppini et al., 1991). These slices have been generated from the cortex, hippocampus, spinal cord, cerebellum and some from the whole brain (Quick et al., 2014, Remuzgo-MartÍnez et al., 2013, Gianinazzi et al., 2005, Kawasaki et al., 2002, Ridoux et al., 1995).

The brain slice model is advantageous because the 3D organizational tissue structure and neuronal network functionality are sustained. The model also provides for direct access and controlled tissue manipulation and indirectly through the extracellular medium. The slice cultures, with their natural variety of the different constitutive cell types, serve as a microcosm of the CNS where the inherent immune response i.e. microglial activation and cytokine/chemokine production, can be investigated in isolation of extracranial immune responses. Moreover, the functional neuronal circuits in the slice can be measured to study the intrinsic properties of neurons including action potentials, membrane potentials and the activity of voltage-gated ion channels.

1.8. Past use of OBSCs in CNS infection studies

The OBSCs have mostly been utilised to investigate parasitic infections of the CNS, the organisms studied include *Trypanosoma brucei brucei* (Stoppini et al., 2000), *Neospora caninum* (Muller et al., 2002), *Toxoplasma gondii* (Scheidegger et al., 2005) and *Naegleria fowleri* (Gianinazzi et al., 2005). Some studies have used bacteria such as *Streptococcus pneumoniae* (Hofer et al., 2012), *Listeria monocytogenes* (Guldimann et al., 2012, Remuzgo-MartÍnez et al., 2013) and virus's namely murine cytomegalovirus (CMV) (Kawasaki et al., 2002) and West Nile virus (WNV) (Quick et al., 2014). Falsig *et al*. (2008) demonstrated prion (a protein)

amplification in an organotypic slice culture assay (POSCA) (Falsig and Aguzzi, 2008). These prions are the causative infectious agents of mammalian transmissible spongiform encephalopathies (TSEs) such as Bovine spongiform encephalopathy (BSE) or "mad cow disease" and Creutzfeldt-Jakob disease in humans. In another study, Johansson *et al*. (2005) used Salmonella lipopolysaccharide (LPS) endotoxins derived from the bacteria *Salmonella abortus equi* to activate hippocampal immune cells, in order to characterize the neurodegenerative effects of LPS as a consequence of the induced neuroinflammation.

1.9. Aims

Based on the previous reports, it is clear that the model of OBSCs is suitable and versatile to address the immunological questions that are pertinent to the understanding of infectious diseases that afflict the CNS of human beings. To date *M. tuberculosis* infection of the CNS has not been explored using organotypic slice cultures. This research thesis will therefore seek to (a) establish and optimize a *M. tuberculosis* infection in OSCs (b) expound any immunological response thereof and (c) investigate the effect of the infection on the intrinsic properties of neurons.

2. MATERIALS AND METHODS

2.1 Mice

C57BL/6 mice were bred and maintained under specific-pathogen free (SPF) conditions at the animal unit located at the basement of the Werner-Beit South building at the Medical School campus of the University of Cape Town (South Africa). The animal unit provided upon request, seven-day old (P7) neonates. All animal experimental protocols complied with South African regulations. Approval was obtained from the Faculty of Health Sciences Animal Research Ethics Committee, University of Cape Town, Cape Town, South Africa (reference numbers AEC 015/012) in accordance with the South African National Standard 10386, *The Care and Use of Animals for Scientific Purposes*.

2.2 Mycobacteria

Bacille Calmette-Guerin-GFP (BCG-GFP) (courtesy of Professor Douglas B. Young, Imperial College of Science, Technology and Medicine) in a 2ml cryotube was retrieved from cryostorage, thawed and emptied into a 1L Conical flask containing 200ml Middlebrook 7H9 broth (Difco Laboratories) [containing 10% oleic acid-albumin-dextrose-catalase (OADC), 0.5% Tween 80 and 50µl/ml hygromycin], which was then incubated at 37°C with shaking for approximately 3 weeks. One millilitre 'stock' aliquots of the 200 ml bacterial culture were aliquoted out and stored at -80°C.

2.3 Bacterial stock concentration

A frozen aliquot was thawed, passed 30 times through a 1ml 29-gauge syringe needle (‘B. Braun’ Omnican Insulin Syringes), and plated in 10-fold serial dilutions onto Middlebrook 7H10 agar half-plates (Difco Laboratories) [containing 10% OADC, 0.5% glycerol and 50µl/ml hygromycin]. These plates were incubated at 37°C for approximately 3 weeks. The concentration of BCG-GFP was then determined by counting the colony forming units (CFU). For this project, one batch of BCG-GFP stock with a calculated concentration of $4.37x10^7$cfu/ml was prepared and used.

2.4 Organotypic slice cultures

Seven-day old mouse pups were collected from the SPF animal unit. The pups were used to generate organotypic hippocampal slice cultures using a preparation method similar to that described by (Stoppini et al., 1991). Briefly, the pups were killed by cervical dislocation using a steel rod, after decapitation the brains were extracted and placed in cold (4°C) ‘dissection media’ [Geys Balanced Salt Solution (GBSS), supplemented with D-glucose (34.7mM)]. All reagents were purchased from Sigma-Aldrich, unless stated otherwise. The hemispheres, in dissection media, were manually separated using a scalpel and individual hippocampi were removed using a thin spatula and immediately sectioned into 350µm thick slices on a McIlwain tissue chopper.

After sectioning, the hippocampi were washed into a 50ml Falcon tube with approximately 5ml of cold ‘dissection media’, the Falcon tube was shaken by hand

to separate out the slices, this also served as a 'rinse'. The separated slices in the Falcon tube were then poured into a small dish, and from there an individual slice was sucked up using a 5ml Pasteur pipette and placed onto a Millicell membrane insert (Merck-Millipore Ltd., Ireland) in a 6-well plate.

The hippocampal slices were then cultivated with 1.2ml of 'growth' media [25% EBSS, 50% MEM, 25% heat-inactivated horse serum, glucose, and B27 (Invitrogen)] which was poured around the insert into the well of the plate i.e. the slices were fed through the porous membrane which was in direct contact with the growth media (Figure 3). The slice cultures were then maintained at 37°C in a 5% CO2 humidified incubator (Nuaire), and given fresh 37°C growth media at 2-day intervals. The slice cultures were viable beyond 14 days post-culture but were not kept past this time point.

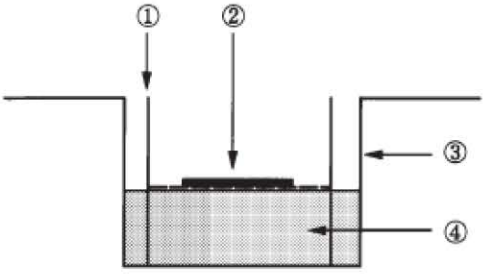

Figure 3: Sketch diagram of an organotypic slice culture. A tissue slice sits on a porous Millicell membrane insert suspended on culture media. (1) insert (2) hippocampal slice (3) well of plate (4) 'growth' media (Shinmura et al., 1999)

2.5 Bacterial infection of slices

For BCG-GFP infection of slices, a BCG-GFP aliquot was retrieved from -80°C, thawed, vortexed briefly and then placed in a eppendorf centrifuge (Centrifuge 5415 R, Eppendorf, Germany). The centrifugation was done at: 10 000rpm for 10 minutes

at 4°C. The supernatant was discarded, leaving behind the bacterial pellet. The pellet was resuspended with 50µl of MEM, vortexed for 3 minutes and passed 30 times through a sterile 1ml 29-gauge syringe needle (‘B.Braun’ Omnican Insulin Syringes).

Twenty-five microlitres was then pipetted out from the 50µl into an eppendorf tube together with 5µl of 1% fast green dye, to make a 30µl BCG-GFP solution. From this dyed 30µl bacterial solution, 2.5µl was loaded into a glass micropipette using a 10ml pipette and a 20µl microloader long tip (Eppendorf, Germany).

The glass micropipette was produced by ‘pulling’ filamental borosilicate glass capillaries (1.2mm outer diameter, 0.69mm inner diameter; Harvard Apparatus Ltd) using a Sutter P-1000 micropipette puller (Sutter Instruments, USA).

The tip of the loaded glass micropipette, under a microscope, was carefully and gently broken on folded tissue paper. A tiny tinge of the green dye appearing on the paper was the indicator that the glass tip had been broken. This loaded micropipette was then coupled to a custom pressure ejection system (Openspritzer) (Forman et al., 2016) and mounted on a Leitz precision micromanipulator (Figure 4A).

The BCG-GFP was injected into the slice by applying multiple bursts (20ms) of pressurized air (approximately 1.4 bar) to the loaded glass micropipette using the Openspritzer; the dye served to show the area of successful injection (Figure 4B). The preparation of mice, generation of hippocampal slice cultures and bacterial infection thereof were all conducted in a biosafety level 2 (BSL 2) tissue culture room.

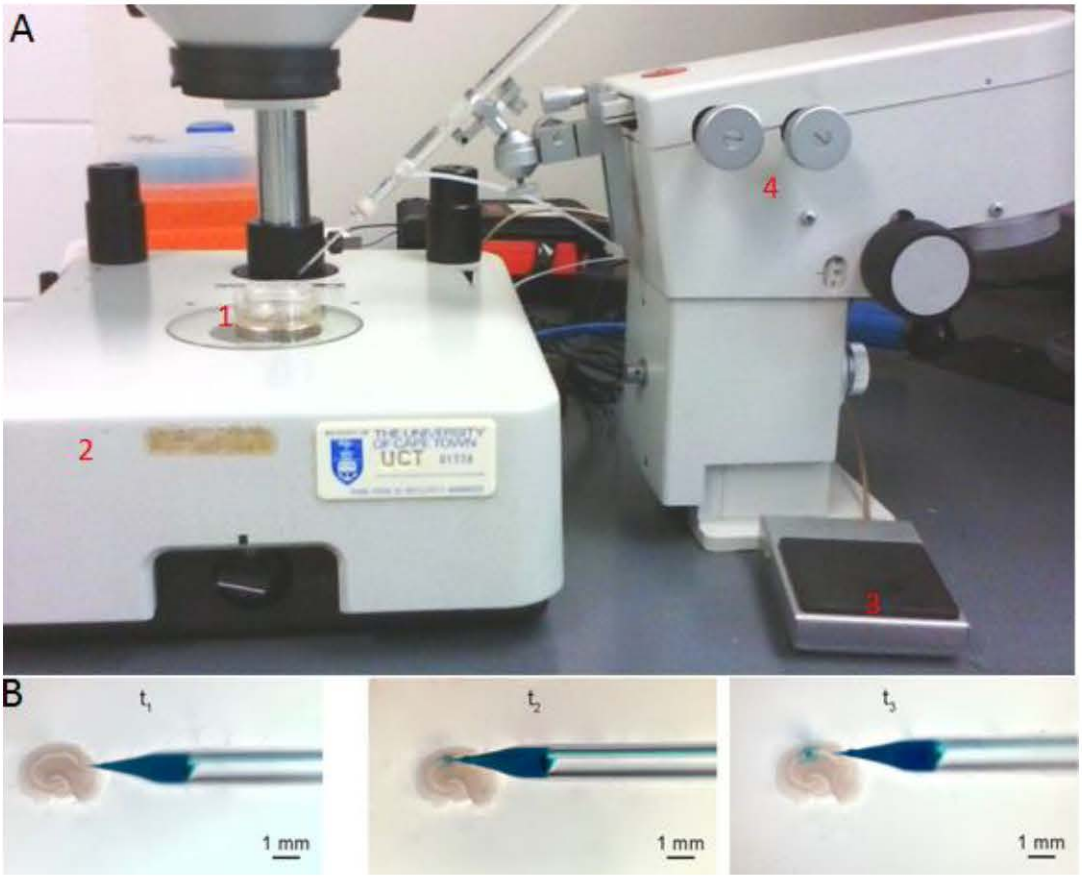

Figure 4: Images of the technique used to infect hippocampal slice cultures with BCG. A) A small petri dish (1) sits atop a stereo microscope (2) the dish contains 'growth' media and a membrane insert with the hippocampal slices. The glass pipette is coupled to a customized pressurized injection system (Openspritzer) (Forman et al., 2016), controlled by a foot pedal (3) and positioned using a micromanipulator (4). B) Serial images of an injection of BCG (and dye) into an organotypic hippocampal slice ($t_1 - t_3$).

2.6 Bacterial CFU from an infected slice

To determine the CFU of BCG-GFP in an individual infected hippocampal slice, the slice was carefully scooped off the insert membrane using a scalpel blade and smeared onto a disposable 0.40µm cell strainer (FALCON, USA). On the strainer, the hippocampal slice was repeatedly mashed through using the back of a plunger of a 1ml syringe with intermittent washing with PBS to a total volume of 1ml. This 1ml homogenate was then plated in 10-fold serial dilutions onto Middlebrook 7H10 agar half-plates (Difco Laboratories) [containing 10% OADC, 0.5% glycerol and 50µl/ml

hygromycin]. These plates were incubated at 37°C for approximately 3 weeks. The BCG-GFP colony forming units per slice were then determined.

2.7 Enzyme-linked Immunosorbent assays (ELISA)

Sandwich ELISAs were conducted to determine the concentration of the following cytokines: IL-1β, IL-6 and IL-10. The supernatant from the cultured organotypic slices was collected at different experimental time points, and was stored at -80°C. Ninety-six well plates (Nunc-immuno maxisorb, Denmark) were coated and incubated overnight (O/N) at 4°C with primary 'capture' antibody diluted in PBS (see appendix 'B' for ELISA antibodies). Between each step the plates were washed 4X with washing buffer and blocked (4% BSA in PBS) O/N at 4°C. Standards and samples were added and incubated at 4°C O/N. The corresponding biotinylated secondary antibody was added and incubated at 37°C for 1 hour. All plates were then incubated at 37°C with Streptavidin coupled to alkaline phosphatase for 1 hour. The optical density (OD) was measured at 405 and 492 nm on a Versamax microplate spectrophotometer (Molecular Devices, Germany).

2.8 Immunofluorescence and Confocal Imaging

Hippocampal slices were briefly rinsed in PBS (pH 7.4) at room temperature (RT), followed by a 15min wash in -20°C methanol. Then a rinse in PBS and were fixed in 4% paraformaldehyde in PBS (pH 7.4) for 1 hour at RT. After washing with PBS, they were incubated at 4°C with blocking buffer (1% BSA in PBS) for 1 hour. Then slices were incubated with a primary antibody in blocking buffer, either a rabbit polyclonal antibody against β-tubulin III (dilution 1:1000), rabbit polyclonal antibody against GFAP (dilution 1:1000) or a goat polyclonal antibody against Iba-1 (dilution 1:500) for 48 hours at 4°C.

After 3X10min rinses with PBS, the slices were incubated O/N at 4°C with a Cy3-conjugated anti-rabbit or donkey anti-goat secondary antibody. Slices were left on the Millicell membrane throughout the whole immunofluorescence-labelling process. The slices were washed in PBS, stained with nuclear marker DAPI in the dark at RT (1:1000 in blocking buffer) for 10min. Slices were rinsed in PBS then mounted with Dako fluorescent mounting media (Dako North America Inc., USA) with the membrane onto the glass slide and tissue facing the cover slip. Z-stack images were captured of the immunofluorescence-labelled slices using a Zeiss 510LSM confocal microscope (Oberkochen, Germany).

2.9 Electrophysiological Recordings

2.9.1. Slice preparation

Hippocampal slices were acquired by cutting the insert membrane around the desired slice using a scalpel and immediately immersed, using forceps, in a small

dish filled with warm oxygenated standard artificial cerebrospinal fluid (aCSF). The slices were then transferred onto the microscope stage on the recording rig, weighed down with a 'U-shaped' wire and continuously superfused with 95%O_2/5% CO_2 aCSF, warmed to 31–34°C. The composition of the "standard" aCSF was as follows: 120 mM NaCl, 3mM KCl, 2mM $MgCl_2$, 2mM $CaCl_2$, 1.2 mM NaH2PO_4, 23mM $NaHCO_3$, and 11 mM D-Glucose. The pH was adjusted with NaOH to be between 7.35 – 7.4.

2.9.2. Patch-clamp recording and analysis

Patch pipettes ('internal electrode') with a tip resistance of 4–7MOhm were pulled from glass capillaries using the Sutter P-1000 micropipette puller (Sutter Instruments, USA). For whole-cell recordings, the pyramidal neurons in the arch between CA3 and CA1 were visualized and targeted for recordings using a 20X water immersion objective (Olympus) on an upright microscope (Olympus BX51WI) equipped with a CCD camera (Mightex, CCE-B013-U) (Figure 3). The 'internal electrode' pipettes were filled with an internal solution containing: 120mM K-gluconate, 0.3mM NaGTP, 4mM Na_2ATP, 10mM Na_2-phosphocreatine, 10mM KCl, and 10mM HEPES. The internal solution had an adjusted osmolarity of 290 mOsm and the pH was adjusted to 7.38 with KOH. Patch-clamp recordings were made using an Axopatch 200B amplifier (Axon Instruments). BCG-GFP was visualized live on the recording rig using a 480nm high powered LED and GFP emission filter set.

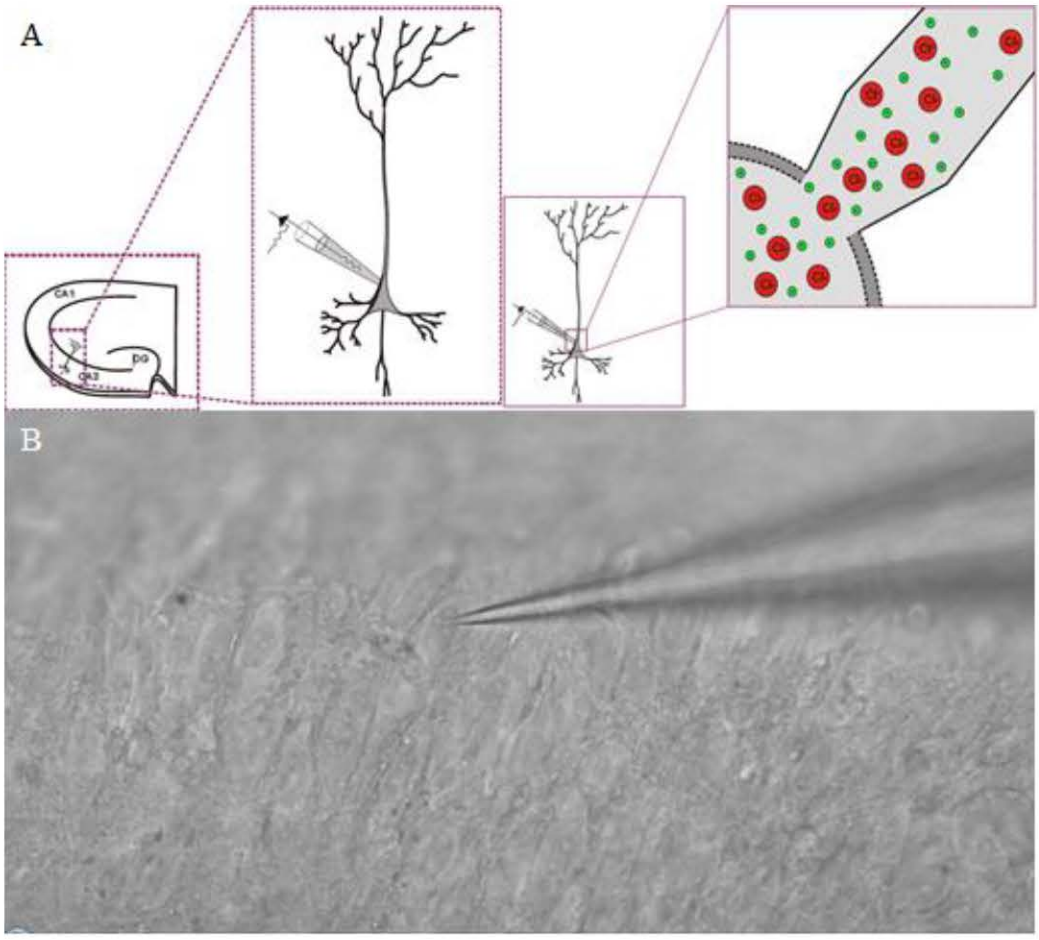

Figure 5: Diagram of a whole-cell patch-clamp recording. A) Left, a schematic representation of the area targeted for recordings (CA3 to CA1). The inset depicts the patch pipette electrode attached to a pyramidal neuron. Right, a successful whole-cell patch-clamp recording entails a continuous connection between the internal solution of the electrode and the cell cytoplasm*. B) A transmitted light image of the CA3 region of an organotypic hippocampal slice. The glass electrode and patched pyramidal neuron are visible. *courtesy of Richard Burman, UCT.

In a subset of experiments, in addition to the patch pipette, a secondary 'puffer' pipette was pulled with the same tip resistance as the patch pipette. This 'puffer' pipette was filled with either 5mM NMDA or 1mg/ml PPD solution which would be 'puffed' directly onto the patched cell using the same pressure injection system as described above (Openspritzer). The timing and duration of puffs were controlled by the WinWCP acquisition software (Figure 6). The NMDA solution had an adjusted osmolarity of 290mOsm/kg and 277mOsm/kg for PPD. These puff experiments

were recorded in the presence of 0.5µM/ml tetrodotoxin (TTX) or TTX+ Glutamate blockers [2mM Kynurenic acid, 20µM CNQX disodium salt hydrate, 100µM D-AP5] added to the standard aCSF to silence endogenous synaptic activity in the slice.

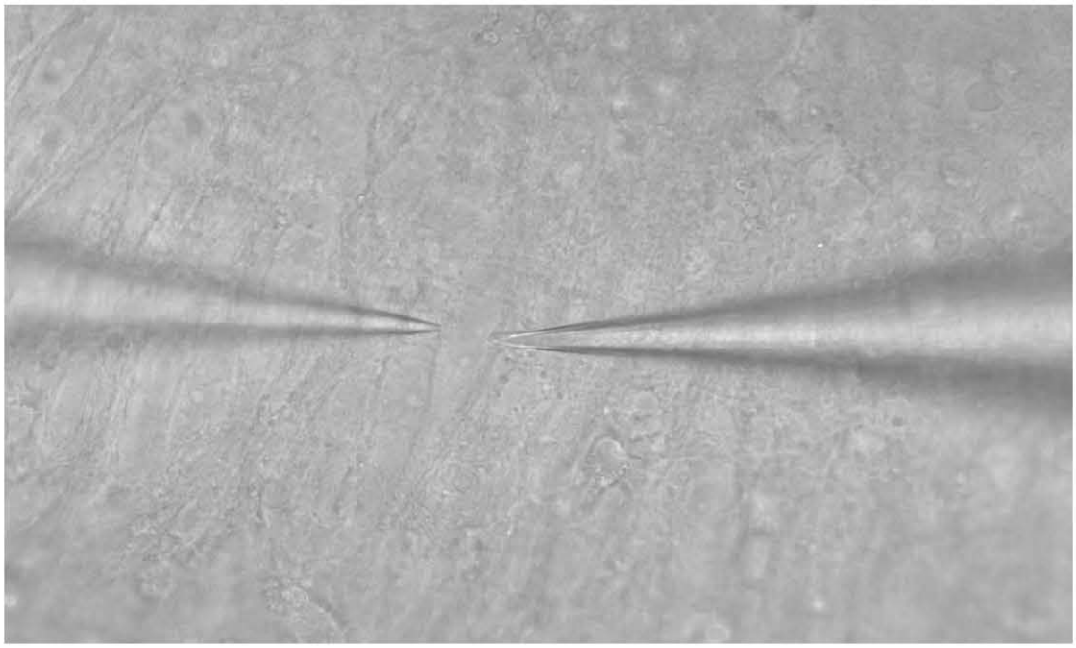

Figure 6: A transmitted light image of pyramidal neurons between the CA3-CA1 region of an organotypic hippocampal slice. Right: the patch pipette, attached to a neuron. Left: the 'puffer' pipette above the patched neuron; the 'puffer' pipette delivers a 'puff' of either NMDA or PPD solution at programmed intervals and duration using the (Openspritzer) pressure injection system controlled by WinWCP acquisition software.

2.10 Statistical analysis

The data was acquired with WinWCP Strathclyde Whole Cell Analysis software (V5.1.4; University of Strathclyde) and then exported to the MATLAB platform (MathWorks) for further analysis using customized scripts. Where appropriate, an unpaired t test with Welch's correction or a 2way ANOVA was used for statistical analysis in GraphPad Prism version 6.01 (GraphPad Software). Data are reported as mean ± SEM or SD. A p-value, $p<0.05$ was considered significant.

3. Results

In a study done by (Randall et al., 2014), the investigators succeeded in demonstrating for the first time that neurons, from established murine cell lines and primary cultures, were able to internalize *M. tuberculosis* bacilli. In their concluding remarks, the researchers indicated that further work was necessary to determine what effect the internalization of *M. tuberculosis* would have on neuronal function.

Neurons possess a few basic measurable properties that affect their functionality in homeostatic conditions which are termed intrinsic properties. These basic properties can be measured prior to or without external stimulation of the neurons and therefore can serve as a good indicator of any impact or difference between a steady-state environment and one with the pathogen *M. tuberculosis.*

Furthermore, the immune response to *M. tuberculosis* in the CNS has been described using many animal models in both *in vivo* and *in vitro* preparations. However the innate immune response in CNS-TB has not been elucidated in the presence of all CNS cell types and functional neural network *in vitro*. So pursuant to investigating CNS-TB in an environment where 'natural' neuroimmune tissue interactions are possible, seven-day old C57BL/6 neonates were used to generate organotypic hippocampal slice cultures. These cultures were then infected with BCG and analysed for immunological and electrophysiological responses to the infection.

3.1 Organotypic hippocampal slices can be moderately infected with BCG

The first objective was to establish an optimal infection protocol of the hippocampal slices and then to quantify the viable BCG-GFP colony forming units (cfu) within an infected slice. The average dimensional lengths of a hippocampal slice (n=9) are shown in (Figure 7A) and the colony forming units in (Figure 7B). The cfu burden of BCG-GFP per slice, 48 hours post-infection, was determined to be approximately 30 cfu per slice. Therefore throughout this project, using the infection protocol outlined in the 'Methods' section, the BCG-GFP infection in OBSCs was established with 30 cfu per slice.

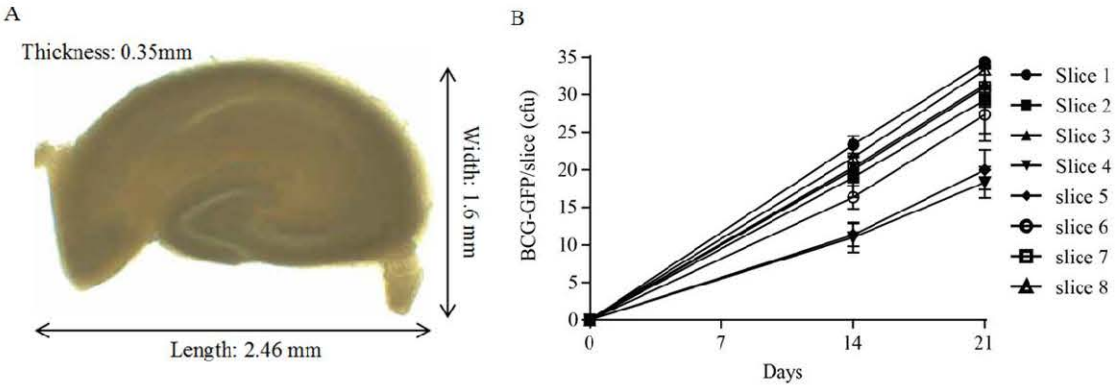

Figure 7: BCG colony forming units in a hippocampal slice. A) The average dimensions of an organotypic hippocampal slice (n=9). B) The cfu count of BCG per slice. Each slice homogenate was serially diluted then plated (in triplicate) 48hrs post-infection and the plates incubated for 21 days. Colonies were counted on day 14 & 21. Data representative of 1 experiment. Values are means ± SEM.

3.2 BCG closely associates with CNS cell types during infection

An advantage of OBSCs as mentioned earlier is the preservation of the 3D-organizational structure of the tissue. The neuron-axon-neuron connections are maintained together with the interspersed and layered presence of other CNS cell types such as astrocytes and microglia. (Randall et al., 2014) were able to demonstrate using fluorescence confocal microscopy the internalization of *M. tuberculosis* bacilli in neurons and microglia from murine cell lines and dissociated primary cultures.

So this study further investigated the association and/or internalization of BCG-GFP in neurons, astrocytes and microglia in organotypic hippocampal slice cultures (Figure 7). The hippocampal slices were allowed 5 days to recover from post-culture trauma and then infected with BCG-GFP using the Openspritzer pressure injection system. The infected slices when then processed for fluorescent confocal microscopy between 2 to 4 days post-infection.

In (Figure 8) the locations of GFP expressing bacilli have shown that the delivery of BCG bacilli varies per area injected and that the overall number of bacilli that remain in a slice is relatively moderate (Figure 7B). The BCG bacilli (green) were observed to be in close association to the βIII-tubulin^{+} pyramidal neurons (red) after incubation for 2 days (Figure 8A, arrows) and 4 days (Figure 8B, arrows) post-infection. Similarly the BCG bacilli were also observed to have close association with GFAP^{+} astrocytes (red) (Figure 8C, arrows). The Iba1^{+} microglial cells (red) were also shown to have a close association with the BCG bacilli (Figures 8D-G, arrows).

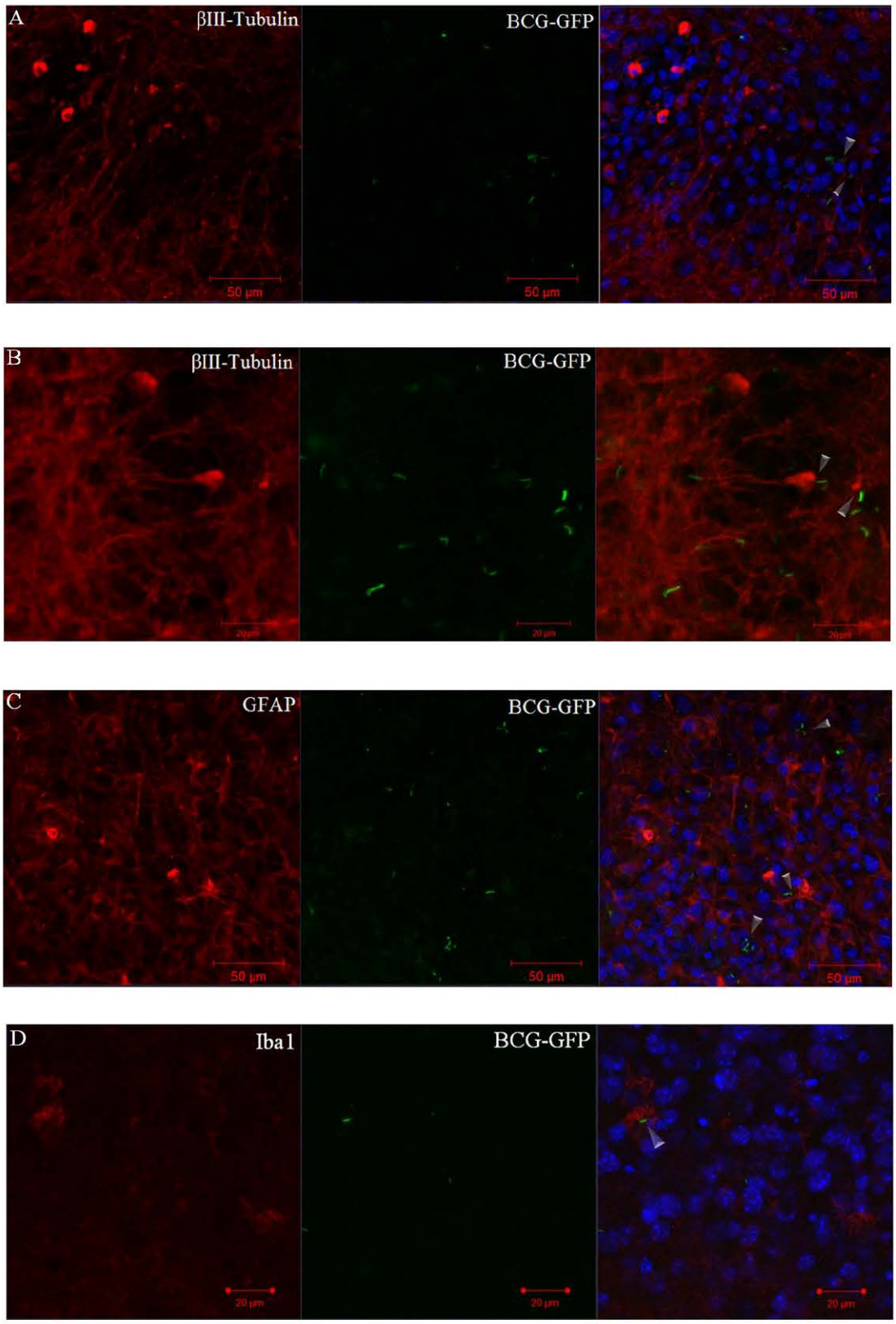
A
βIII-Tubulin
BCG-GFP
50 μm
50 μm
50 μm
B
βIII-Tubulin
BCG-GFP
20 μm
20 μm
20 μm
C
GFAP
BCG-GFP
50 μm
50 μm
50 μm
D
Iba1
BCG-GFP
20 μm
20 μm
20 μm

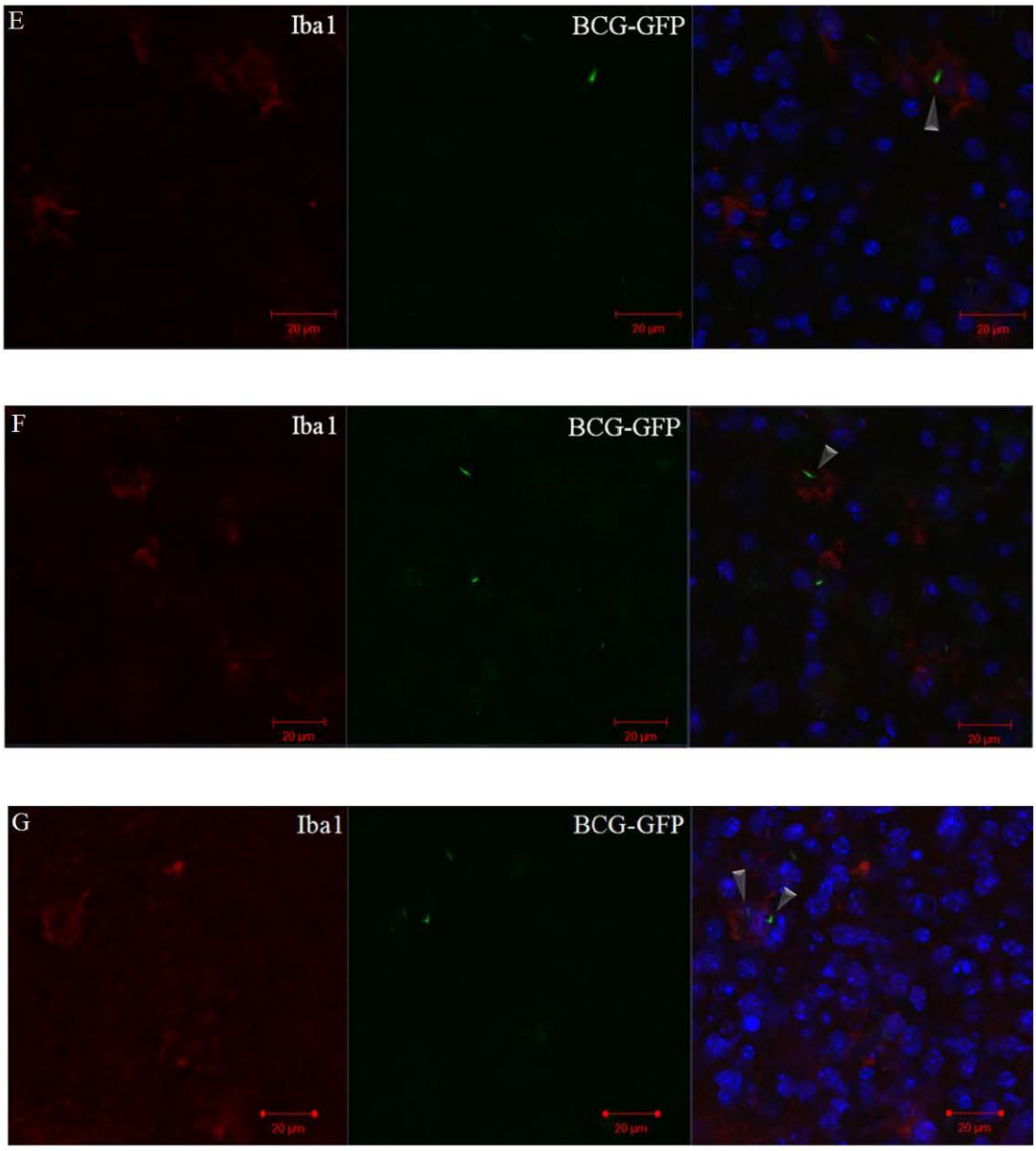

Figure 8: BCG associates with neurons, astrocytes and microglial cells. Murine organotypic hippocampal slice cultures established using 7 day-old C57BL/6 neonates were infected with ~30 cfu of BCG-GFP bacilli (green) per slice. All nuclei were stained with DAPI (blue) and the images captured by confocal microscopy using 40X water immersion objective. The neurons were stained with β (III)-Tubulin (red) (A-B) 2 and 4 days post-infection. The astrocytes (C) were stained with GFAP (red) 4 days-post infection. The microglial cells were stained with Iba1 (red) 3 days (D-E) and 4 days (F-G) post-infection. Scale bars: 20 and 50µm.

3.3 BCG does not produce a distinguishable immune response

(Remuzgo-MartÍnez et al., 2013) demonstrated that an infection with *L. monocytogenes* in 300µm thick rat organotypic whole-brain slices produced a quantifiable increase of the cytokines IL-1β and IL-6. So this study investigated whether or not a BCG infection of organotypic hippocampal slice cultures would produce a quantifiable immune response. To this end, the hippocampal slices were allowed to recover from culturing trauma for 5 days and then were infected with BCG. The supernatants from the cultures were collected 24hrs post-culturing, 24hr and 48hrs post-infection together with the corresponding non-infected time points.

The supernatants were analysed by ELISA to measure the amounts present of the cytokines IL-1β, IL-6 and IL-10 (Figure 9). The quantities for all 3 cytokines respectively, remained unchanged from what they were 24hrs post-culturing. Therefore the BCG infection did not stimulate a distinguishable immune response in the slices.

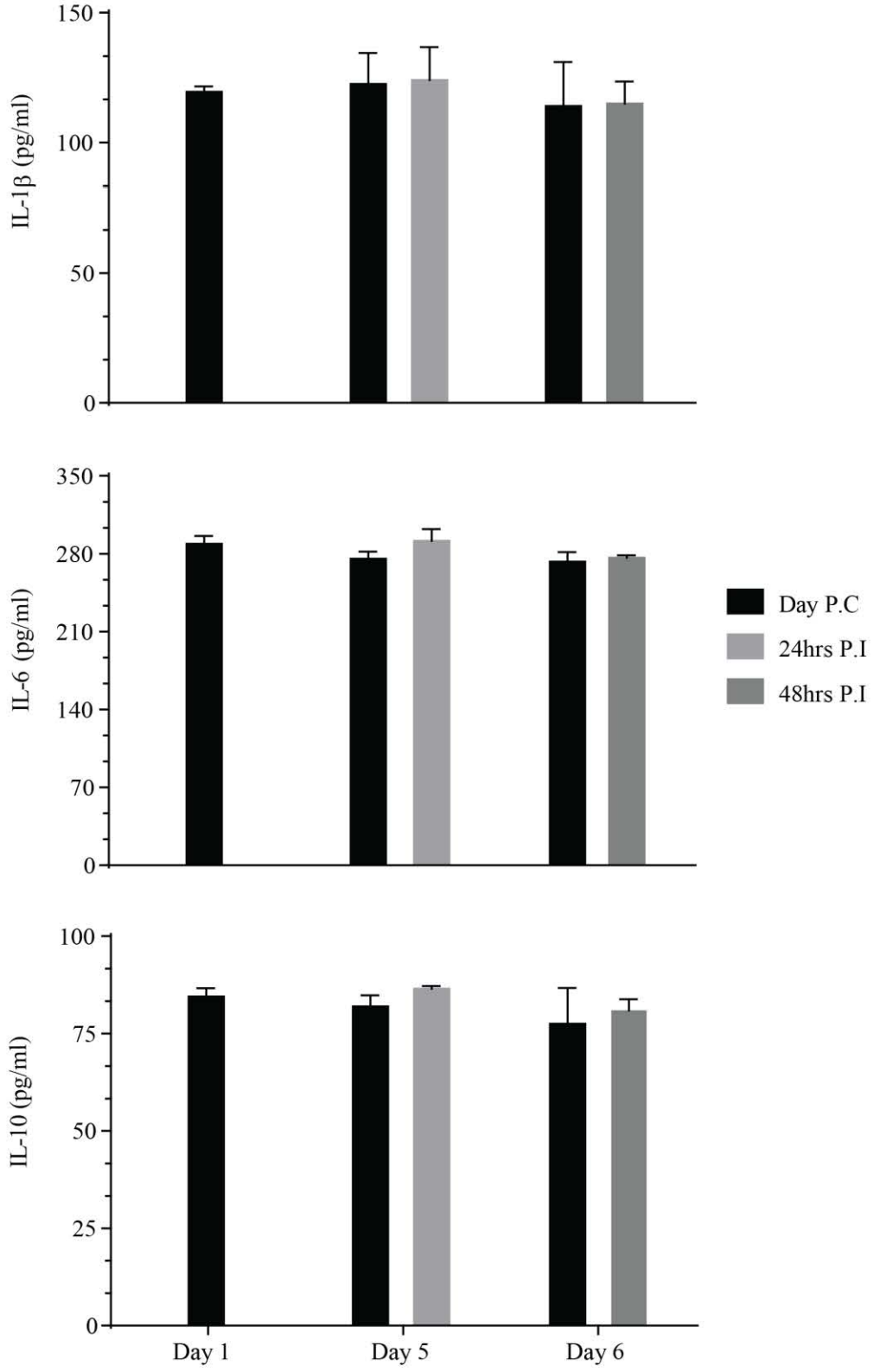

Figure 9: BCG does not elicit an immune response in hippocampal slices. Supernatants from organotypic hippocampal slice cultures were analysed (in duplicate) by ELISA to quantify the amounts of the cytokines IL-1β, 6 and 10. The supernatants were collected at these time points: 24hrs post-culturing (P.C) (Day 1), 24 and 48hrs post-BCG infection (P.I) with the corresponding P.C days. Data representative of 2 experiments. Values ± SEM.

To investigate the effect, if any, of a mycobacterial infection on neuronal function, the hippocampal slice cultures were infected with BCG-GFP. The conjugated green fluorescent protein in the bacteria enabled visualization of the bacilli in the slice under blue light on the recording rig (Figure 10). The bacteria were injected along the CA3-CA1 'band' of pyramidal neurons in the hope that some bacilli might be internalized by these neurons. However, if not internalized, the test was to determine whether or not the close proximity of the bacilli had any measurable effect on neuronal function, in particular the intrinsic properties.

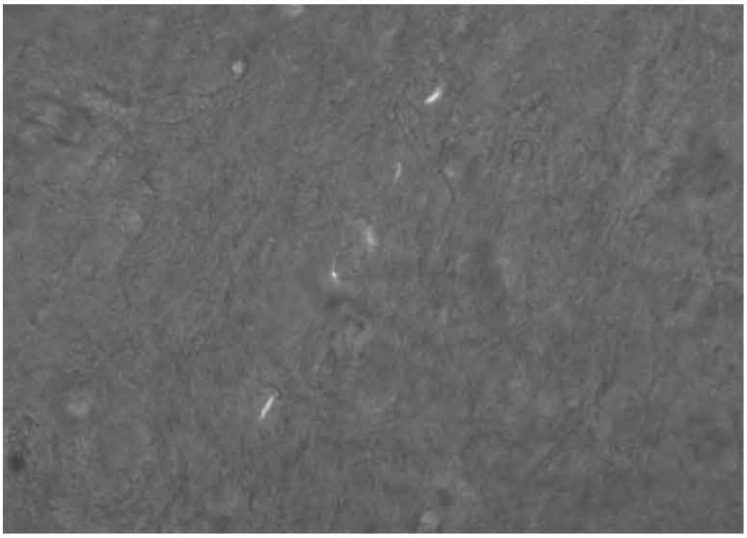

Figure 10: BCG-GFP bacilli in an organotypic hippocampal slice generated from seven-day old 57BL/6 neonates 24 hours post-infection, visualized using a 480 nm high powered LED and a GFP filter set on the recording rig.

3.4.1. BCG infection has no effect on the membrane properties of neurons

The basic membrane properties including the membrane resistance, membrane capacitance and the resting membrane potential comprise the fundamental properties that modulate the signalling of neurons. As such these membrane properties are a good starting to point to determine how an infection affects the functioning of neurons.

To determine if the membrane properties of neurons were affected in a non-homeostatic state, hippocampal slice cultures were infected with BCG-GFP and the pyramidal neurons from these infected slices were whole-cell patched, analysed and compared to non-infected slices (Figure 11).

The measurement of the adequacy of the patch 'seal', the average Ra (access resistance), and population comparison thereof between infected and non-infected slices (Figure 11A) was not significantly different (p=0.83, unpaired t test). The mean for the non-infected slices was 25.77 ± 5.83mOhm (n=14) and 26.30 ± 7.51mOhm (n=17) for the BCG-infected slices. This was an important outcome because all subsequent neuronal properties and parameters are influenced by how well the 'seal' is formed i.e. the continuation of the cytoplasm with the internal solution of the patch 'internal' electrode is important for electrical conductance. Following the formation of a proper seal, and prior to any external stimulation, the membrane resistance, membrane capacitance and the resting potential were recorded (Figures 11B-D). These three properties, respectively, indicate the 'health' of the cell, the amount of charge stored by and size of the bi-lipid membrane, and lastly the voltage across the membrane.

Respectively for each figure, the means for the non-infected slices were 116.5 ± 40.39mOhm (n=14), 196.1 ± 48.37pF (n=16) and -62.04 ± 5.01mV (n=17). Correspondingly, for the BCG infected slices 98.17 ± 24.95mOhm (n=16), 161.5 ± 49.31pF (n=17) and -62.60 ± 4.88mV (n=18). The means for all three figures respectively, were statistically not significant (p=0.15; p=0.051; p=0.74; all unpaired t tests). The measured properties in (Figure 11) taken collectively indicate that the BCG infection of hippocampal slices did not alter the basic membrane properties of the neurons.

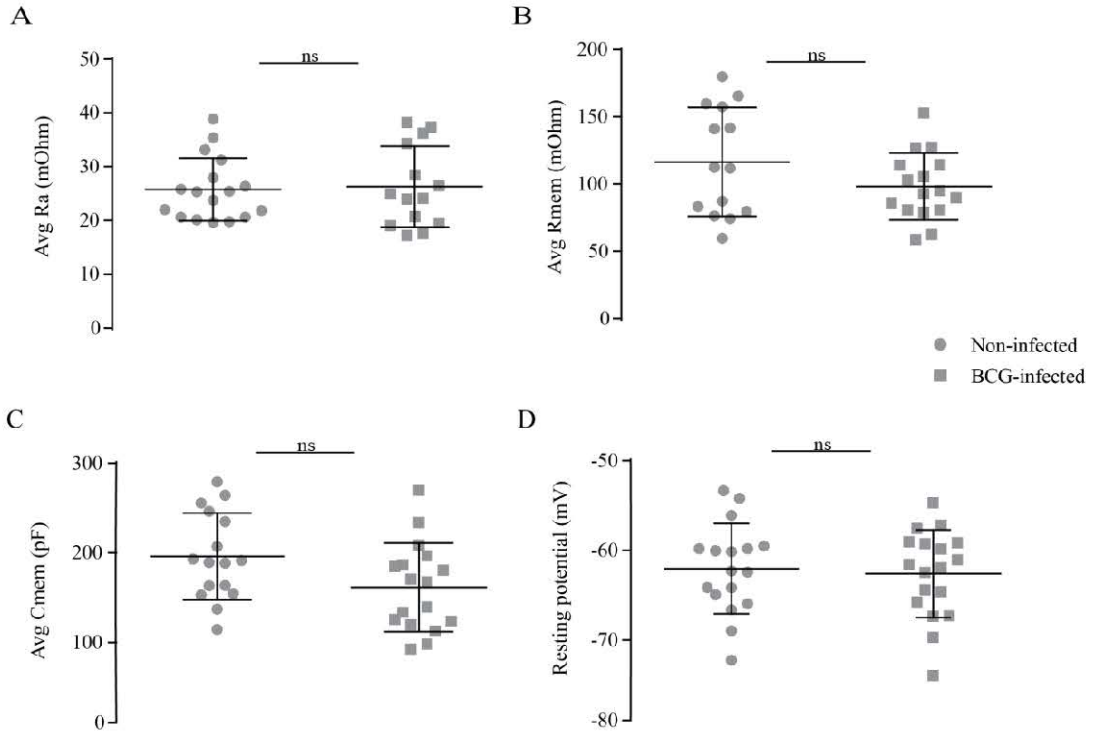

Figure 11: BCG does not alter the membrane properties of hippocampal neurons. Whole-cell patch recordings were made from CA3-CA1 pyramidal neurons in control & BCG-infected organotypic hippocampal slice. The average Ra values, access resistance, which is a measure of the quality of the whole-cell patch-clamp recording, were similar between the two conditions (A). The average membrane resistance (B), average membrane capacitance (C) and the resting membrane potential (D) were not significantly different between the two groups. Values with means ± SD; $p<0.05$, ns = not significant.

3.4.2. BCG infection of does not change neuronal intrinsic excitability

Neurons communicate and modulate one another by generating and releasing action potentials or 'spikes'. Thus a change in the ability or propensity of a neuron to release an action potential may have significant consequences for a local neural circuit or network. To investigate what effect, if any, the presence of BCG bacilli would have on the generation of action potentials by neurons in infected hippocampal slice cultures (Figure 12).

The hippocampal CA3-CA1 pyramidal neurons from infected and non-infected (control) slices showed no significant difference (p=0.69, unpaired t test) between the threshold voltage at which an action potential would be generated. In (Figure 12A) the stimulus protocol (incremental current injections of 10pA for 500ms) utilized to elicit the first action potential showed that a current injection of 130pA for 500 ms sufficiently depolarized the neuron down to its action potential threshold of -40.36mV whereupon the first 'spike' was released. The mean population threshold voltage for control slices was -38.72 ± 5.45mV (n=17), comapred to -39.54 ± 5.86mV (n=14) for the BCG-infected slices (Figure 11B).

Furthermore, the current density threshold, the amount of current required to elicit a spike normalized by membrane capacitance, was also not significantly different (p=0.35, unpaired t test) between the control and BCG-infected slices (Figure 12B). The mean in non-infected slices was 0.83 ± 0.17 pA/pF (n=15) and 0.75 ± 0.27 pA/pF (n=12) in BCG-infected slices. This is an important outcome because it indicates that the patched neurons were of similar intrinsic excitability between the two groups.

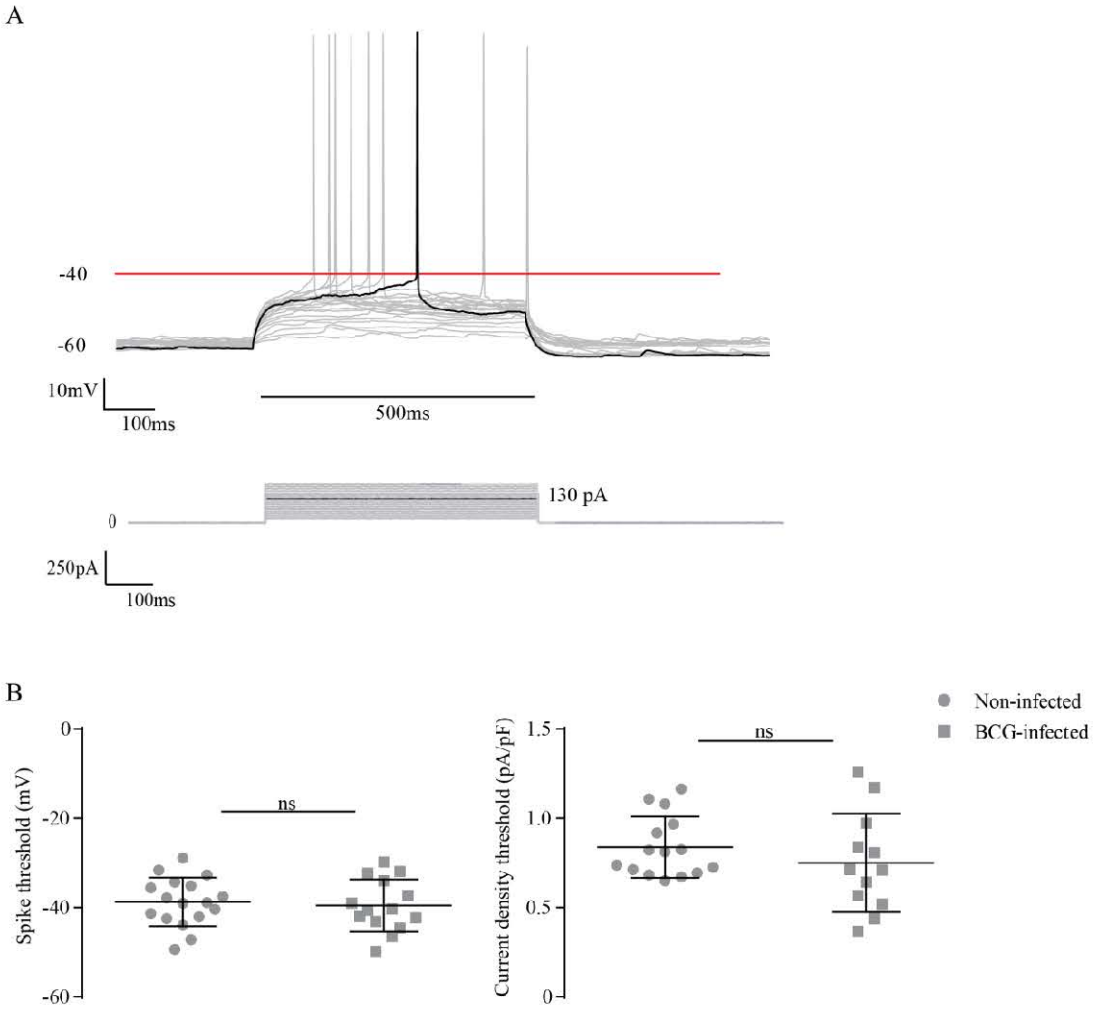

Figure 12: BCG infection has no effect on the 'spike' threshold of hippocampal neurons. A) The first 'spike' generated by a neuron reveals an action potential threshold 0f -40.36mV. This occurred following the injection of 130pA of current for 500ms. B) Left, the spike threshold population data recorded from whole-cell patched CA3 pyramidal neurons demonstrates no difference in the spike threshold between non-infected vs BCG-infected organotypic hippocampal slices. Right, the current density threshold was also not significantly different between the two groups. Values with means ± SD; $p<0.05$, ns = not significant.

3.4.3. BCG infection does not alter the maximum spiking rate of neurons

The rate or frequency with which neurons are able to 'spike' is an important element of maintaining a functional neural signalling network. The effect of a sudden and transiently sustained heightening of the 'spiking' frequency of neurons can be readily observed in the neurological disorder of epilepsy.

The effect, if any, on the spiking frequency of neurons in BCG-infected hippocampal slice cultures was investigated (Figure 13). The results showed that there was no significant difference over the first 500ms (p=0.87, t test) and the maximum spiking rate (p=0.61, t test), respectively, of neurons between infected and non-infected hippocampal slice cultures. In (Figure 13A) the current clamp traces showing the maximum 'spiking' frequency of pyramidal neurons between non-infected (i) and BCG-infected (ii) hippocampal slices. The maximum 'spike' rate was observed after the current injection of 300pA and 200pA for 1500ms, respectively. The bars above each trace indicate 500ms and the spike frequency in that time, 34Hz and 36Hz respectively. (Figure 13B) shows the population data of the mean spiking rate for the first 500ms had a mean of 21.33 ± 7.53Hz (n=18) for non-infected slices and 21.83 ± 10.52Hz (n=18) for the BCG-infected slices. Then the maximum 'spiking' frequency i.e. 1/shortest time between successive spikes, was 57.22 ± 35.37Hz the (n=18) and 62.90 ± 30.70Hz (n=18) in BCG-infected slices.

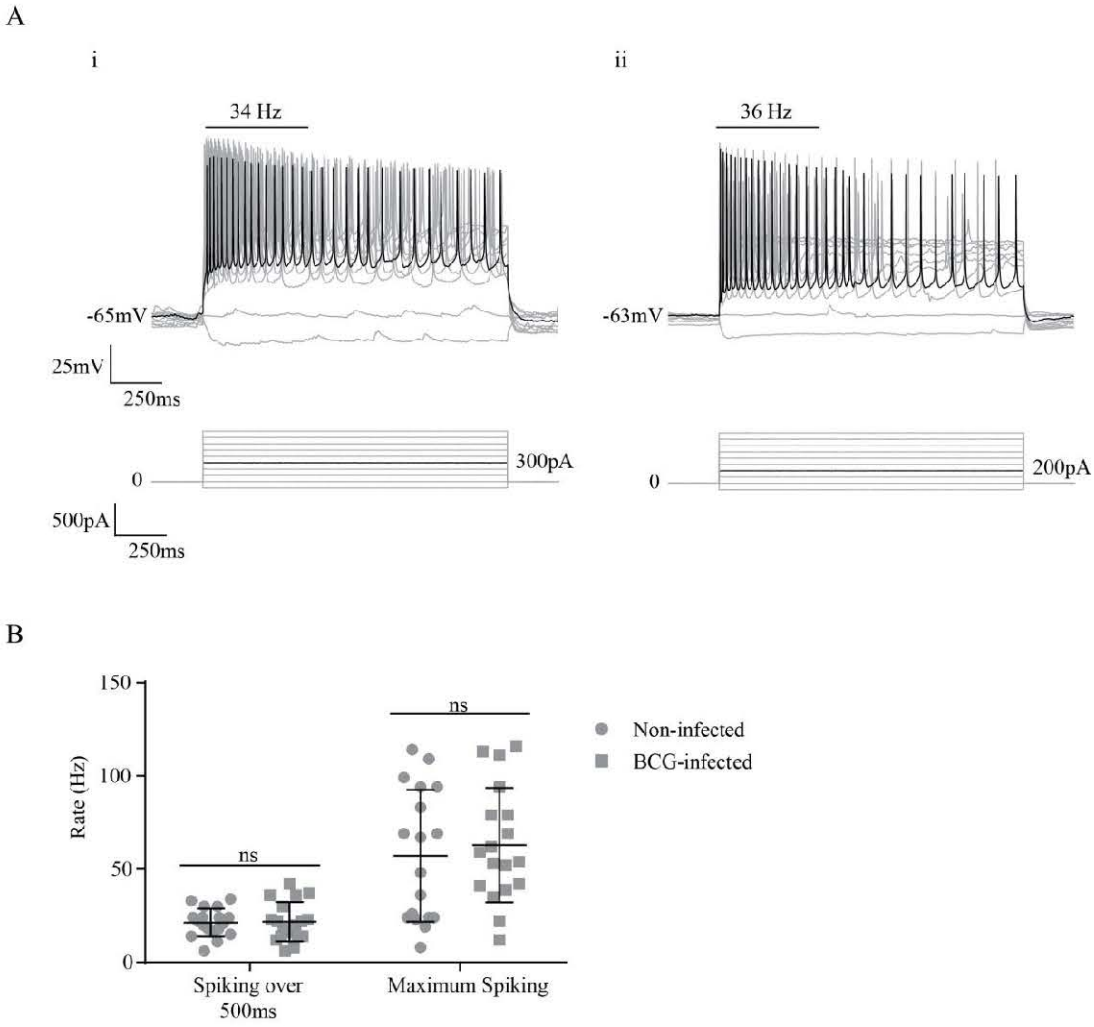

Figure 13: BCG infection does not alter the maximum 'spike' rate of pyramidal neurons. The maximum 'spike' rate population data recorded from whole-cell patches on CA3 pyramidal neurons in organotypic hippocampal slices. A) The current clamp traces showing the maximum 'spiking' frequency of pyramidal neurons between non-infected (i) and BCG-infected (ii) hippocampal slices. The maximum 'spike' rate was observed after the current injection of 300pA and 200pA for 1500ms, respectively. The bars above each trace indicate 500ms with the spike frequency in that time, 34Hz and 36Hz respectively. B)The population data recorded from whole-cell patched CA3 pyramidal neurons demonstrates no difference in the mean spiking rate over 500ms and the maximum spiking rate (1/shortest time between successive spikes) between non-infected vs BCG-infected organotypic hippocampal slices. Values with mean ± SD; $p<0.05$, ns=not significant.

3.4.4. BCG does not alter the magnitude of ion channel currents

The membrane of neuronal cells contain ion channels at varying degrees of concentration. The flux of ion currents through these channels modulates the electrical signalling of a neuron. The activity of three ion currents namely, I_{Na}^{+}, I_{K}^{+} and I_A were recorded and analysed to see if BCG infection had any effect on ion channel activity (Figure 14). The I_{Na}^{+} current is mediated by voltage-gated Na channels and the I_{K}^{+} current is largely a function of the passive K leak channels. Lastly, the I_A current is generated by voltage-gated K channels involved in repolarization following an action potential.

The results showed that there was no significant difference in the flow (magnitude) of ion currents over all three ion channels post-BCG infection, (I_{Na}, I_K, I_A; p=0.62, 0.84, 0.59). The stimulus protocols for each ion current (Figure 14 Ai-ii) were recorded from CA3 pyramidal neurons in infected hippocampal organotypic slices. The maximum current amplitudes were determined over a specified time window. Whole-cell patched neurons produced a maximum I_{Na}^{+} ion current of -3546pA and I_A of 1050 following a voltage-clamp at -20mV for less than 0.01s (i). The maximum I_{K}^{+} ion current was 1640pA following a voltage-clamp at 10mV for 1000ms (ii). In (Figure 14B) the population data and means of the maximum ion currents I_{Na}, I_K, I_A respectively, were -3241.14 ± 1135.55pA, 1459.48 ± 534.94pA, 1094.03 ± 422.68pA (n=18) for non-infected slices and -3476.70 ± 1678.6pA, 1503.44 ± 816.48pA, 1181.79 ± 552.61pA (n=18) for BCG-infected slices, respectively. Collectively, this demonstrates that BCG infection of hippocampal slices does not alter ion currents.

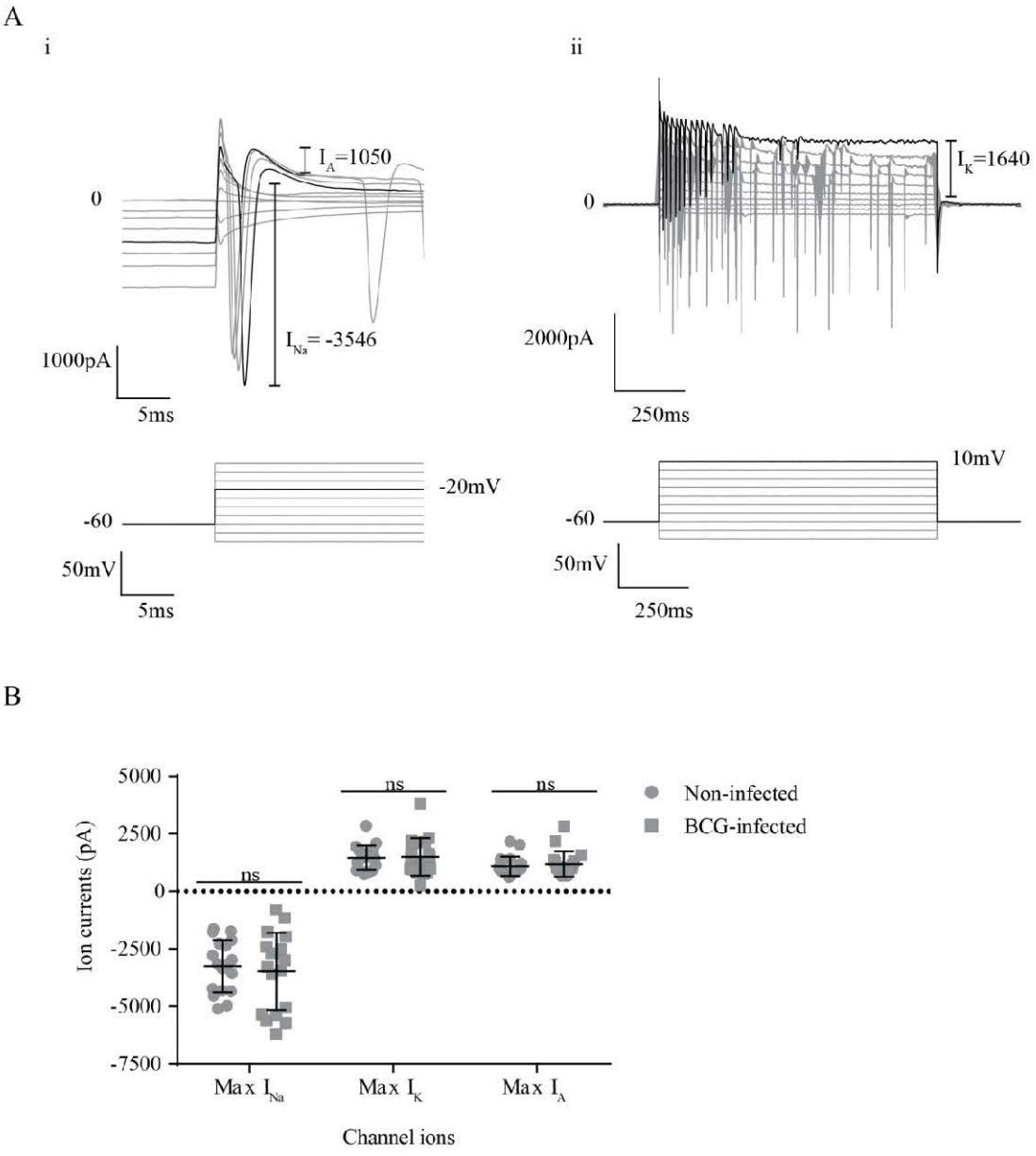

Figure 14: BCG infection does not affect the flow (magnitude) of ion currents. The ion currents (INa+, IK+, IA) were measured from whole-cell patched CA3 pyramidal neurons in organotypic hippocampal slices. A) The maximum INa & IA ion currents (i) from BCG-infected slices following a voltage clamp at -20mV for less than 0.01s and the maximum IK ion current (ii) following a voltage-clamp at 10mV for 1000ms. B) The population data of all three ion currents demonstrated no significant difference between whole-cell patched CA3 pyramidal neurons in non-infected vs. BCG-infected organotypic hippocampal slices. Values with means ± SD; $p<0.05$, ns = not significant.

3.4.5. Tuberculin PPD transiently depolarizes CA3 hippocampal neurons

In addition to the injection of BCG bacilli into organotypic hippocampal slices and recording what effect, if any, this would have on neuronal function and properties, a Tuberculin PPD solution (*Mycobacterium tuberculosis* extract) was 'puffed' directly onto whole-cell patched pyramidal neurons and measured the effect.

The non-infected hippocampal slices were immersed and continuously superfused with oxygenated aCSF with 0.5µM TTX added to it. The neurons were 'puffed' with 50mM NMDA (positive control) in aCSF-TTX, 1mg/ml PPD in aCSF-TTX and 1mg/ml PPD in aCSF-TTX + Glutamate blockers [2mM Kynurenic acid, 20µM CNQX disodium salt hydrate, 100µM D-AP5] and lastly, standard aCSF (negative control) in aCSF-TTX. At the reported concentrations reported these antagonists should block NMDA, AMPA and kainite receptors, the three major classes of glutamate receptor. In (Figure 15A) representative traces of each 'puff' experiment were recorded 500ms after commencement. All puff experiments were performed at each cell's particular resting membrane potential. As all responses were depolarizing, small differences in driving force created by different holding potentials may have affected the size of measured voltage responses to PPD, but not the existence of the responses in the first place.

In (Figure 15B) the population data of NMDA (positive control) produced large depolarization potentials with a mean of 9.33 ± 2.07mV (n=6), as expected. The 'puff' of PPD in aCSF-TTX caused a mean depolarization potential that was significantly smaller than the positive control but which were statistically significant compared to 'puffs' of standard aCSF 1.80 ± 1.11mV (n=5, p=0.027 unpaired t test). The 'puff' of PPD in aCSF-TTX-Glut Block was not significantly different

from just aCSF-TTX 2.26 ± 1.17mV (n=4, p=0.56 unpaired t test). The negative control caused a negligible mean depolarization of 0.11 ± 0.04mV (n=5). These results demonstrated that the Tuberculin PPD causes a moderate and transient depolarization of the membrane potential of hippocampal pyramidal neurons.

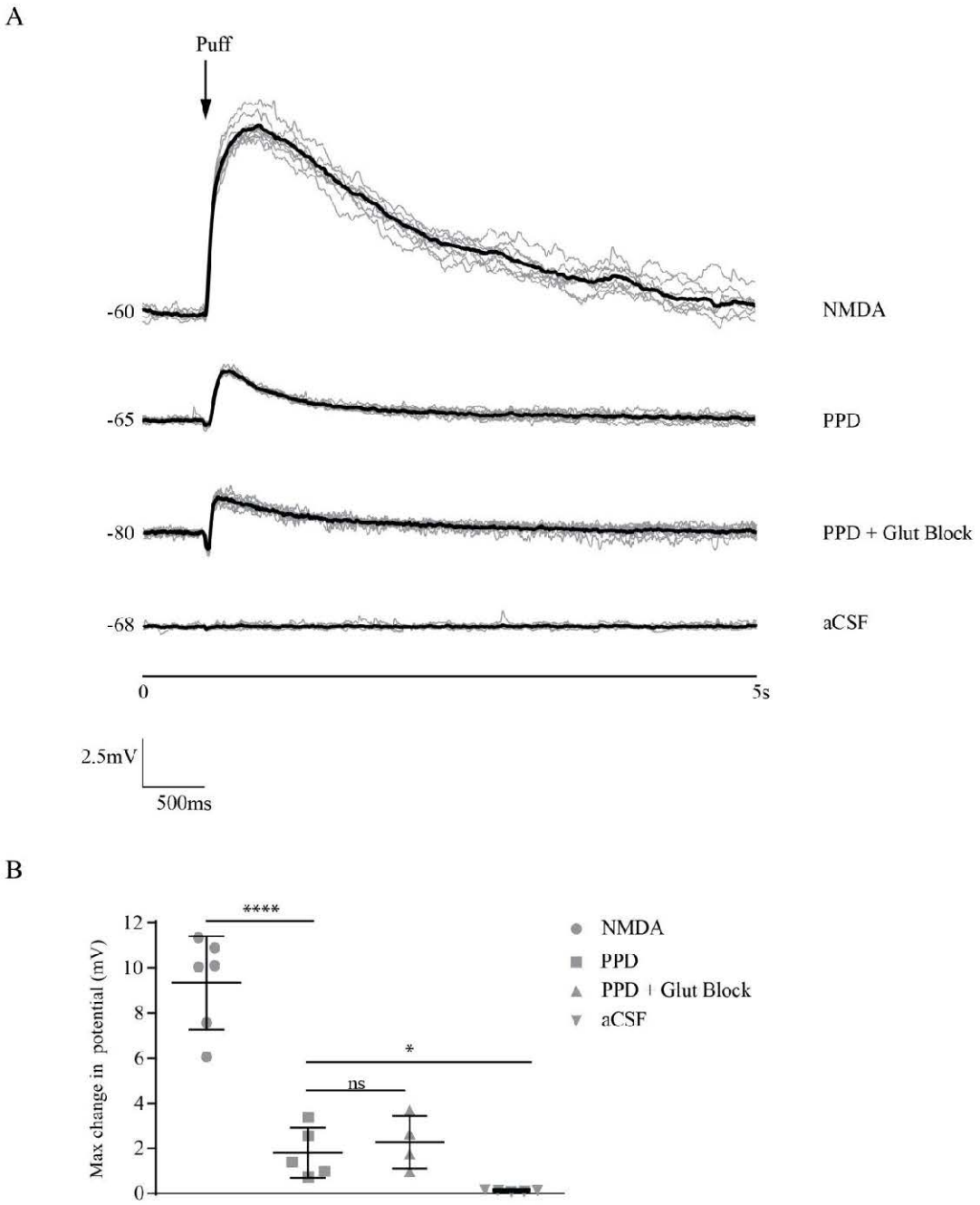

Figure 15: Tuberculin PPD moderately and transiently depolarizes neurons. The maximum change in potential recorded from whole-cell 'puff' patches on CA3 pyramidal neurons in organotypic hippocampal slices. A) Representative traces of each 'puff' experiment. B) The population data of 5mM NMDA (positive control), 1mg/ml PPD and standard aCSF (negative control) 'puffed' directly onto neurons that were continually superfused with either aCSF-TTX(0.5μM) or aCSF-TTX+ Glutamate blockers 500ms into each recording lasting 5s. The PPD 'puff' was statistically significant compared to the negative control. However, the 'puff' of PPD in both types of aCSF were not significant when compared to each other. Values with means ± SD; $p<0.05$,ns=not significant.

4. Discussion

Tuberculosis (TB) of the central nervous system (CNS-TB) is an infection of the nervous tissue with the bacterium *Mycobacterium tuberculosis*. This pathological condition is fairly rare, accounting for approximately 5% of all extra-pulmonary TB, however, it is characterized by high morbidity and mortality, especially during childhood and in immunosuppressed individuals. Notwithstanding the seriousness of CNS-TB, most research is still focussed on elucidating the pathology and immune response interplay in the pulmonary form of the disease. This is seen in the few publications that explore the nexus of immunological and neuroelectrophysiological effects of a *M. tuberculosis* infection of the CNS, indeed (Randall et al., 2014) were the first ever to demonstrate that *M. tuberculosis* bacilli can be internalized by neurons. The novelty of demonstrating neurons as a target for *M. tuberculosis* infection has, naturally, raised more questions than answers concerning CNS-TB. One outstanding question is the potential impact an infection has on the properties and function of neurons.

To investigate the implications of an *M. tuberculosis* infection on neuronal properties and functions, the model of organotypic hippocampal slice cultures was used. First, an optimal bacterial infection in the hippocampal slices was established. Then, the infected slice cultures were analysed to determine the immune response elicited focussing on the production of the cytokines IL-1β, IL-6 and IL-10. To observe the interaction of the bacteria with the CNS cell types, immunohistochemistry and confocal microscopy was conducted on the infected slice cultures, labelling for neurons, astrocytes and microglia.

Lastly the whole-cell patch clamp technique was used to investigate the effect of the bacterial infection in hippocampal slices on the intrinsic properties and function of neurons. The fluorescent microscopy revealed BCG bacilli in close proximity to neurons, astrocytes and microglia. The immune response elicited post-BCG infection was not distinguishable from uninfected slice cultures. Moreover, BCG infection of hippocampal slice cultures had no measurable effect on the intrinsic properties of neurons. However, Tuberculin purified protein derivative (PPD) did produce a depolarizing change in the resting membrane potential of pyramidal neurons. Therefore, taken together the data generated from both immunological and electrophysiological analysis, demonstrates that BCG infection of hippocampal slice cultures produces to minimal to no changes in cytokine production and neuronal intrinsic properties.

Seven day old C57BL/6 mice were used to generate organotypic hippocampal slice cultures as similarly described by (Stoppini et al., 1991). The hippocampal slices were infected with BCG of differing concentrations using the Openspritzer pressure injection system (Forman et al., 2016) and the slices were homogenized, plated in 10-fold serial dilutions and incubated at 37°C for 21 days. At the incubation time points (day 14 & 21) the BCG cfu were calculated. An average of 30cfu was the highest concentration of the BCG bacilli that could be achieved (Figure 7B). The reason for this modest infection could be due to several factors: (a) the size of the slices (b) delivery by pressure injection (c) short time for infection (d) the doubling time of BCG. The hippocampal slices are quite small in size (Figure 7A) and this meant the surface area available for infection with the glass pipette was limited because tissue damage from repeated insertion in sites close to one another had to be

avoided. In addition continued injection would result in the bacterial solution not being retained in the slice i.e. it would either flow through the slice and out, or track back up the injection site and out. The slices were also infected on the benchtop in the tissue culture room (BSL2) which was kept clean however this necessitated that the slices be infected in a short time to avoid contamination with airborne particles. Moreover no antibiotic was included in the feeding media because this adversely affected the health of the slices i.e. it shortened the time slices could be maintained in culture. The most crucial factor that determined the cfu count was the doubling time of BCG. BCG has a doubling time of 20-23hrs which is significantly greater than the previously utilized bacteria in this model such as *L. monocytogenes*: 45-60min (Guldimann et al., 2012, Guldimann et al., 2015) or *S. pneumoniae*: 20-30min (Hofer et al., 2012). Therefore, all of the above factors potentially attribute to the low bacterial burden found in the BCG-infected organotypic hippocampal slice cultures. That said we were able to confirm and quantify a successful infection of the hippocampal slices with BCG.

To observe the interaction of BCG-GFP with the cell types of the CNS, the hippocampal slices were immunolabelled for neurons, astrocytes and microglia. BCG was observed to associate with all the labelled cell types (Figure 8). (Randall et al., 2014) demonstrated a *M. tuberculosis*-to-neuron association percentage of 21% after 48hrs in dissociated neuron primary cultures infected with a multiples of infection (MOI) ratio of 30:1. They also reported an internalization percentage in the same primary cultures with the same MOI of approximately 11% after 24hrs of infection. The BCG-neuron association was not calculated in this study but was observed (Figure 8A, B). No obvious internalization of BCG-GFP into neurons could be observed in the slice cultures. A probable reason for the lack of

internalization was that the ratio of BCG to neurons in these slices was far smaller compared to the dissociated primary cultures. Furthermore, the presence of other 'intervening' cell types in the slices may have contributed to not only the low observed close proximity of the bacilli to the neurons but may have been a significant determinant for the lack of internalization.

Astrocytes have long since been described to play an active and important role in innate immunity (Dong and Benveniste, 2001, Rock et al., 2005, Farina et al., 2007) which includes secretion of pro-inflammatory cytokines and neurotrophic factors. The BCG-GFP bacilli were only observed to be closely associated with astrocytes (Figure 8C). This is consistent with past findings where (Rock et al., 2005) reported only a 15% cell-association of astrocytes with virulent *M. tuberculosis* in human primary cultures. Moreover, astrocyte colonization may be largely affected by the type of pathogen used as *T. gondii* (a parasite) overwhelmingly infected astrocytes in rat cortical slices, leaving microglia and neurons mostly unaffected (Scheidegger et al., 2005) similarly with *N caninum* (Vonlaufen et al., 2002). However, the low BCG burden attained in these hippocampal slices may also be a major factor for the lack of internalization.

Microglia, the residential immune cells are known to be the primary target of *M. tuberculosis* in CNS-TB infection (Curto et al., 2004, Rock et al., 2005). The BCG-GFP was seen in close association with the microglia (Figures 8D-G). Furthermore, microglia were not only observed in all sites of BCG-GFP inoculation but also proximal to nearly all BCG bacilli throughout the slice. However, no clearly visible internalization was observed. In contrast, (Guldimann et al., 2015) reported a vast majority of *L. monocytogenes* bacilli grew within microglia in bovine organotypic slices, albeit the slices had a high bacterial load. So again the modest presence of

BCG in the hippocampal slices together with the characteristic non-pathogenic and non-virulent makeup of the bacilli may be the reasons for the apparent lack of phagocytic activity.

The immune response post-BCG infection in hippocampal slices was assessed using ELISA. BCG infection of organotypic hippocampal slice cultures did not produce a distinguishable immune response with respect to the secretion of cytokines IL-1β, IL-6 and IL-10 (Figure 9). The assayed cytokines showed sustained levels from the 24hrs post-culture to the two time points post-infection. This result was in contrast to (Remuzgo-MartÍnez et al., 2013) who had previously demonstrated an increase in the production of IL-1β and IL-6 on rat whole-brain organotypic slice cultures after an infection with *L. monocytogenes* and similarly, an increase in IL-6 was demonstrated in spinal cord slices infected with WNV by (Quick et al., 2014), although this was with a high viral load inoculum. Moreover, the virulent *M. tuberculosis* lab strain H37Rv was able to elicit increased IL-1β, IL-6 and IL-10 production in murine primary neural cultures (Randall et al., 2014). Therefore, the difference in immune response in these hippocampal slices may be explained by (a) the low bacterial burden and (b) non-pathogenicity of BCG.

Infections of the CNS, bacterial meningitis as the most common, are serious conditions that in many cases result in short or long term neurological sequelae ranging from temporary deafness to chronic epilepsy (Perny et al., 2016, Nataprawira et al., 2016, Lucas et al., 2016, Hosoglu et al., 2002, Grimwood et al., 1995). These sequelae may be due to physical tissue damage or perhaps as a consequence of the immune response or both. Therefore it is imperative that CNS infections be investigated.

Hippocampal slice cultures were infected with BCG in order to determine what effect the bacilli had on neuronal function, specifically the intrinsic properties. The intrinsic properties of neurons are the basic measurable parameters of neurons in steady-state conditions. These properties include the membrane resistance, membrane capacitance, resting membrane potential, current density threshold, action potential 'spike' threshold, maximum 'spiking' rate and ion channel currents (flow of ions). Neuroinflammation has been shown to play a crucial role in the pathology of neurodegenerative diseases (McGeer and McGeer, 1995). Pathogens and pro-inflammatory mediators released by immune effector cells, induce neurotoxicity resulting in neuronal necrotic death (Johansson et al., 2005) which naturally disrupts neuronal signalling. I found that BCG infection in hippocampal slice cultures had no effect on the intrinsic properties of neurons (Figures 11-14). This is similar to the lack of effect on the signalling of neurons during *T. brucei brucei* infection in hippocampal slices (Stoppini et al., 2000). Possibly, this is because the BCG bacterial burden was low and therefore did not significantly induce neuroinflammation in the infected slices. An alternative explanation is that neurons have evolved to maintain their function (i.e. ensure intrinsic properties are unperturbed) when challenged with a mild to moderate infection.

As an alternative to the injection of whole bacilli into the hippocampal slices, an isotonic 1mg/ml solution of Tuberculin PPD (*M. tuberculosis* extract) was 'puffed' directly onto patched neurons in non-infected slices and observed the effect (Figure 8). This PPD concentration is the same as that which is intradermally injected into patients. The PPD solution produced a small and transient depolarization of the membrane potential. The solvent for tuberculin PPD is phosphate-buffer saline solution.

A possible explanation for this depolarization effect was that some tuberculin proteins may have broken down into amino acids which include glutamic acid, of which the neurotransmitter glutamate is an anion. However this depolarization effect was reproduced when PPD was 'puffed' onto neurons constantly superfused with aCSF containing TTX (Na^+ ion channel blocker) and glutamate blockers. Therefore, tuberculin PPD transiently depolarizes the membrane potential but the cause for this effect remains unknown. It may be that other depolarizing receptors are being activated e.g. nicotinic acetylcholine receptors or acid sensing ion channels. Future work might use blockers for these receptors to determine their roles.

4.1 Concluding remarks and future work

I successfully utilized BCG infection of organotypic hippocampal slice cultures as a model of CNS-TB. In this model I demonstrated that BCG bacilli did not cause a distinguished effect on cytokine production nor on the intrinsic properties of hippocampal neurons. More broadly, BCG infection did not result in observable effects on immune or neuronal function. This lack of effect was possibly due, in part, to the non-virulence of BCG. I did however observe a direct depolarizing effect of tuberculin PPD on neurons which warrants further investigation.

To overcome the abovementioned limitations, future work could utilize a virulent strain of *M. tuberculosis* such as the lab strain H37Rv. This would necessitate the use of a patch-clamping apparatus in a BSL3 environment. Finally, it may also prove valuable to investigate the effect of mycobacteria on neurons by using primary dissociated cultures where neurons with internalized bacilli can be directly observed and targeted for whole-cell patch-clamp recordings. Moreover, the infection load might be improved by using younger pups and infecting them at earlier time point.

5. References

<Global TB report 2015.pdf>.

BE, N. A., KIM, K. S., BISHAI, W. R. & JAIN, S. K. 2009. Pathogenesis of central nervous system tuberculosis. *Curr Mol Med,* 9**,** 94-9.

BE, N. A., LAMICHHANE, G., GROSSET, J., TYAGI, S., CHENG, Q. J., KIM, K. S., BISHAI, W. R. & JAIN, S. K. 2008. Murine model to study the invasion and survival of Mycobacterium tuberculosis in the central nervous system. *J Infect Dis,* 198**,** 1520-8.

BECK, H. & YAARI, Y. 2008. Plasticity of intrinsic neuronal properties in CNS disorders. *Nat Rev Neurosci,* 9**,** 357-69.

BEDFORD, H., DE LOUVOIS, J., HALKET, S., PECKHAM, C., HURLEY, R. & HARVEY, D. 2001. Meningitis in infancy in England and Wales: follow up at age 5 years. *BMJ,* 323**,** 533-6.

BERENGUER, J., MORENO, S., LAGUNA, F., VICENTE, T., ADRADOS, M., ORTEGA, A., GONZALEZ-LAHOZ, J. & BOUZA, E. 1992. Tuberculous meningitis in patients infected with the human immunodeficiency virus. *N Engl J Med,* 326**,** 668-72.

BERMUDEZ, L. E. & GOODMAN, J. 1996. Mycobacterium tuberculosis invades and replicates within type II alveolar cells. *Infect Immun,* 64**,** 1400-6.

BURNS, M. E. & AUGUSTINE, G. J. 1995. Synaptic structure and function: dynamic organization yields architectural precision. *Cell,* 83**,** 187-94.

CHRISTIE, B. R. & CAMERON, H. A. 2006. Neurogenesis in the adult hippocampus. *Hippocampus,* 16**,** 199-207.

CURTO, M., REALI, C., PALMIERI, G., SCINTU, F., SCHIVO, M. L., SOGOS, V., MARCIALIS, M. A., ENNAS, M. G., SCHWARZ, H., POZZI, G. & GREMO, F. 2004. Inhibition of cytokines expression in human microglia infected by virulent and non-virulent mycobacteria. *Neurochem Int,* 44**,** 381-92.

DONALD, P. R., SCHAAF, H. S. & SCHOEMAN, J. F. 2005. Tuberculous meningitis and miliary tuberculosis: the Rich focus revisited. *J Infect,* 50**,** 193-5.

DONG, Y. & BENVENISTE, E. N. 2001. Immune function of astrocytes. *Glia,* 36**,** 180-90.

FALSIG, J. & AGUZZI, A. 2008. The prion organotypic slice culture assay[mdash]POSCA. *Nat. Protocols,* 3**,** 555-562.

FARER, L. S., LOWELL, A. M. & MEADOR, M. P. 1979. Extrapulmonary tuberculosis in the United States. *Am J Epidemiol,* 109**,** 205-17.

FARINA, C., ALOISI, F. & MEINL, E. 2007. Astrocytes are active players in cerebral innate immunity. *Trends Immunol,* 28**,** 138-45.

FORMAN, C. J., TOMES, H., MBOBO, B., BADEN, T. & RAIMONDO, J. V. 2016. Openspritzer: an open hardware pressure ejection system for reliably delivering picolitre volumes. *bioRxiv*.

GIANINAZZI, C., SCHILD, M., MULLER, N., LEIB, S. L., SIMON, F., NUNEZ, S., JOSS, P. & GOTTSTEIN, B. 2005. Organotypic slice cultures from rat brain tissue: a new approach for Naegleria fowleri CNS infection in vitro. *Parasitology,* 131**,** 797-804.

GINHOUX, F., GRETER, M., LEBOEUF, M., NANDI, S., SEE, P., GOKHAN, S., MEHLER, M. F., CONWAY, S. J., NG, L. G., STANLEY, E. R., SAMOKHVALOV, I. M. & MERAD, M. 2010. Fate mapping analysis reveals that adult microglia derive from primitive macrophages. *Science,* 330**,** 841-5.

GRIMWOOD, K., ANDERSON, P., ANDERSON, V., TAN, L. & NOLAN, T. 2000. Twelve year outcomes following bacterial meningitis: further evidence for persisting effects. *Arch Dis Child,* 83**,** 111-6.

GRIMWOOD, K., ANDERSON, V. A., BOND, L., CATROPPA, C., HORE, R. L., KEIR, E. H., NOLAN, T. & ROBERTON, D. M. 1995. Adverse outcomes of bacterial meningitis in school-age survivors. *Pediatrics,* 95**,** 646-56.

GULDIMANN, C., BARTSCHI, M., FREY, J., ZURBRIGGEN, A., SEUBERLICH, T. & OEVERMANN, A. 2015. Increased spread and replication efficiency of Listeria monocytogenes in organotypic brain-slices is related to multilocus variable number of tandem repeat analysis (MLVA) complex. *BMC Microbiol,* 15**,** 134.

GULDIMANN, C., LEJEUNE, B., HOFER, S., LEIB, S. L., FREY, J., ZURBRIGGEN, A., SEUBERLICH, T. & OEVERMANN, A. 2012. Ruminant organotypic brain-slice cultures as a model for the investigation of CNS listeriosis. *Int J Exp Pathol,* 93**,** 259-68.

HESS, D. C., ABE, T., HILL, W. D., STUDDARD, A. M., CAROTHERS, J., MASUYA, M., FLEMING, P. A., DRAKE, C. J. & OGAWA, M. 2004. Hematopoietic origin of microglial and perivascular cells in brain. *Exp Neurol,* 186**,** 134-44.

HOFER, S., MAGLOIRE, V., STREIT, J. & LEIB, S. L. 2012. Grafted Neuronal Precursor Cells Differentiate and Integrate in Injured Hippocampus in Experimental Pneumococcal Meningitis. *STEM STEM CELLS,* 30**,** 1206-1215.

HOSOGLU, S., GEYIK, M. F., BALIK, I., AYGEN, B., EROL, S., AYGENCEL, T. G., MERT, A., SALTOGLU, N., DOKMETAS, I., FELEK, S., SUNBUL, M., IRMAK, H., AYDIN, K., KOKOGLU, O. F., UCMAK, H., ALTINDIS, M. & LOEB, M. 2002. Predictors of outcome in patients with tuberculous meningitis. *Int J Tuberc Lung Dis,* 6**,** 64-70.

JOHANSSON, S., BOHMAN, S., RADESATER, A. C., OBERG, C. & LUTHMAN, J. 2005. Salmonella lipopolysaccharide (LPS) mediated neurodegeneration in hippocampal slice cultures. *Neurotox Res,* 8**,** 207-20.

KAWASAKI, H., KOSUGI, I., ARAI, Y. & TSUTSUI, Y. 2002. The Amount of Immature Glial Cells in Organotypic Brain Slices Determines the Susceptibility to Murine Cytomegalovirus Infection. *Laboratory Investigation,* 82**,** 1347-1358.

KREUTZBERG, G. W. 1996. Microglia: a sensor for pathological events in the CNS. *Trends Neurosci,* 19**,** 312-8.

LEE, J., LING, C., KOSMALSKI, M. M., HULSEBERG, P., SCHREIBER, H. A., SANDOR, M. & FABRY, Z. Intracerebral Mycobacterium bovis bacilli Calmette–Guerin infection-induced immune responses in the CNS. *Journal of Neuroimmunology,* 213**,** 112-122.

LEUNER, B. & GOULD, E. 2010. Structural plasticity and hippocampal function. *Annu Rev Psychol,* 61**,** 111-40, C1-3.

LUCAS, M. J., BROUWER, M. C. & VAN DE BEEK, D. 2016. Neurological sequelae of bacterial meningitis. *J Infect,* 73**,** 18-27.

MCGEER, P. L. & MCGEER, E. G. 1995. The inflammatory response system of brain: implications for therapy of Alzheimer and other neurodegenerative diseases. *Brain Res Brain Res Rev,* 21**,** 195-218.

MEGIAS, M., EMRI, Z., FREUND, T. F. & GULYAS, A. I. 2001. Total number and distribution of inhibitory and excitatory synapses on hippocampal CA1 pyramidal cells. *Neuroscience,* 102**,** 527-40.

MERKELBACH, S., SITTINGER, H., SCHWEIZER, I. & MULLER, M. 2000. Cognitive outcome after bacterial meningitis. *Acta Neurol Scand,* 102**,** 118-23.

MULLER, N., VONLAUFEN, N., GIANINAZZI, C., LEIB, S. L. & HEMPHILL, A. 2002. Application of real-time fluorescent PCR for quantitative assessment of Neospora caninum infections in organotypic slice cultures of rat central nervous system tissue. *J Clin Microbiol,* 40**,** 252-5.

NATAPRAWIRA, H. M., RUSLIANTI, V., SOLEK, P., HAWANI, D., MILANTI, M., ANGGRAENI, R., MEMED, F. S. & KARTIKA, A. 2016. Outcome of tuberculous meningitis in children: the first comprehensive retrospective cohort study in Indonesia. *Int J Tuberc Lung Dis,* 20**,** 909-14.

NIMMERJAHN, A., KIRCHHOFF, F. & HELMCHEN, F. 2005. Resting microglial cells are highly dynamic surveillants of brain parenchyma in vivo. *Science,* 308**,** 1314-8.

PERNY, M., ROCCIO, M., GRANDGIRARD, D., SOLYGA, M., SENN, P. & LEIB, S. L. 2016. The Severity of Infection Determines the Localization of Damage and Extent of Sensorineural Hearing Loss in Experimental Pneumococcal Meningitis. *J Neurosci,* 36**,** 7740-9.

QUICK, E. D., LESER, J. S., CLARKE, P. & TYLER, K. L. 2014. Activation of intrinsic immune responses and microglial phagocytosis in an ex vivo spinal cord slice culture model of West Nile virus infection. *J Virol,* 88**,** 13005-14.

RANDALL, P. J., HSU, N. J., LANG, D., COOPER, S., SEBESHO, B., ALLIE, N., KEETON, R., FRANCISCO, N. M., SALIE, S., LABUSCHAGNE, A., QUESNIAUX, V., RYFFEL, B., KELLAWAY, L. & JACOBS, M. 2014. Neurons are host cells for Mycobacterium tuberculosis. *Infect Immun,* 82**,** 1880-90.

REMUZGO-MARTÍNEZ, S., PILARES-ORTEGA, L., ICARDO, J. M., VALDIZÁN, E. M., VARGAS, V. I., PAZOS, Á. & RAMOS-VIVAS, J. 2013. Microglial activation and expression of immune-related genes in a rat ex vivo nervous system model after infection with Listeria monocytogenes. *GLIA Glia,* 61**,** 611-622.

RICH, A. & MCCORDOCK, H. 1933. The pathogenesis of tuberculous meningitis. *Bull. John Hopkins Hosp.,* 52**,** 5 - 37.

RIDOUX, V., ROBERT, J., PERRICAUDET, M., MALLET, J. & LE GAL LA SALLE, G. 1995. Adenovirus mediated gene transfer in organotypic brain slices. *Neurobiol Dis,* 2**,** 49-54.

ROCK, R. B., GEKKER, G., HU, S., SHENG, W. S., CHEERAN, M., LOKENSGARD, J. R. & PETERSON, P. K. 2004. Role of microglia in central nervous system infections. *Clin Microbiol Rev,* 17**,** 942-64, table of contents.

ROCK, R. B., HU, S., GEKKER, G., SHENG, W. S., MAY, B., KAPUR, V. & PETERSON, P. K. 2005. Mycobacterium tuberculosis-induced cytokine and chemokine expression by human microglia and astrocytes: effects of dexamethasone. *J Infect Dis,* 192**,** 2054-8.

ROCK, R. B., OLIN, M., BAKER, C. A., MOLITOR, T. W. & PETERSON, P. K. 2008. Central nervous system tuberculosis: pathogenesis and clinical aspects. *Clin Microbiol Rev,* 21**,** 243-61, table of contents.

SCHEIDEGGER, A., VONLAUFEN, N., NAGULESWARAN, A., GIANINAZZI, C., MULLER, N., LEIB, S. L. & HEMPHILL, A. 2005. Differential effects of interferon-gamma and tumor necrosis factor-alpha on Toxoplasma gondii proliferation in organotypic rat brain slice cultures. *J Parasitol,* 91**,** 307-15.

SHINMURA, Y., KOSUGI, I., KANETA, M. & TSUTSUI, Y. 1999. Migration of virus-infected neuronal cells in cerebral slice cultures of developing mouse brains after in vitro infection with murine cytomegalovirus. *Acta Neuropathol,* 98**,** 590-6.

SPANOS, J. P., HSU, N. J. & JACOBS, M. 2015. Microglia are crucial regulators of neuro-immunity during central nervous system tuberculosis. *Front Cell Neurosci,* 9**,** 182.

STOPPINI, L., BUCHS, P. A., BRUN, R., MULLER, D., DUPORT, S., PARISI, L. & SEEBECK, T. 2000. Infection of organotypic slice cultures from rat central nervous tissue with Trypanosoma brucei brucei. *Int J Med Microbiol,* 290**,** 105-13.

STOPPINI, L., BUCHS, P. A. & MULLER, D. 1991. A simple method for organotypic cultures of nervous tissue. *J Neurosci Methods,* 37**,** 173-82.

TSENOVA, L., BERGTOLD, A., FREEDMAN, V. H., YOUNG, R. A. & KAPLAN, G. 1999. Tumor necrosis factor alpha is a determinant of pathogenesis and disease progression in mycobacterial infection in the central nervous system. *Proc Natl Acad Sci U S A,* 96**,** 5657-62.

VONLAUFEN, N., GIANINAZZI, C., MÜLLER, N., SIMON, F., BJÖRKMAN, C., JUNGI, T. W., LEIB, S. L. & HEMPHILL, A. 2002. Infection of organotypic slice cultures from rat central nervous tissue with Neospora caninum: an alternative approach to study host-parasite interactions. *International journal for parasitology,* 32**,** 533-42.

6. Appendices

Appendix A: Solutions

PBS (10X)

80g NaCl (1.37M)

2g KCI (0.03M)

14.4g H_2 $P0_4$ (0.01 M)

2.4g KH_2P0_4

Dissolve in 1 L ddH20

Dilution Buffer

10g BSA (1 %)

0.2g NaN_3 (0.02 %)

Make up to 1 L with 1 X PBS

Substrate Buffer

0.2g NaN_3 (0.02 %)

97 ml di-ethanolamine

0.8g $MgCI_2.6H_20$

700 ml ddH_20

Adjust the pH to 9.8 with 10M HCL and make up to 1 L with ddH_20

Washing buffer (20X)

20g KCL

20g KH_2P04

144g $NA_2HP0_4.H_20$

800g NaCl

50 ml Tween 20

100 ml 10 % NaN_3

Make up to 5 L with ddH_20

aCSF (10X)

NaCl 70.13g

KCl 2.24g

Sodium Bicarbonate 1.87g

D-Glucose 19.32g

Sodium phosphate monobasic dihydrate 19.82g

Add dH_20 to make up to (not add) 1000ml, stir well and refrigerate.

Appendix B: Cytokine/ Antibody ELISA

	Capture	Detection	Standard
IL-1β	4µg/ml	400ng/ml	4ng/ml
IL-6	2 µg/ml	400ng/ml	2ng/ml
IL-10	2 µg/ml	200ng/ml	8ng/ml
Type	Rat anti-mouse	Biotinylated goat anti-mouse	Recombinant
Company	R&D Systems	R&D Systems	R&D Systems

Appendix C: Recording rig